



**HAL**  
open science

## **Rho1- and Pkc1-dependent phosphorylation of the F-BAR protein Syp1 contributes to septin ring assembly**

Laura Merlini, Alessio Bolognesi, Maria Angeles Juanes, Franck Vandermoere, Thibault Courtellemont, Roberta Pascolutti, Martial Séveno, Yves Barral, Simonetta Piatti

### ► To cite this version:

Laura Merlini, Alessio Bolognesi, Maria Angeles Juanes, Franck Vandermoere, Thibault Courtellemont, et al.. Rho1- and Pkc1-dependent phosphorylation of the F-BAR protein Syp1 contributes to septin ring assembly. *Molecular Biology of the Cell*, 2015, 26 (18), pp.3245-3262. 10.1091/mbc.e15-06-0366 . hal-01883492

**HAL Id: hal-01883492**

**<https://hal.science/hal-01883492>**

Submitted on 12 Mar 2020

**HAL** is a multi-disciplinary open access archive for the deposit and dissemination of scientific research documents, whether they are published or not. The documents may come from teaching and research institutions in France or abroad, or from public or private research centers.

L'archive ouverte pluridisciplinaire **HAL**, est destinée au dépôt et à la diffusion de documents scientifiques de niveau recherche, publiés ou non, émanant des établissements d'enseignement et de recherche français ou étrangers, des laboratoires publics ou privés.



Distributed under a Creative Commons Attribution - NonCommercial - ShareAlike 4.0 International License

# Rho1- and Pkc1-dependent phosphorylation of the F-BAR protein Syp1 contributes to septin ring assembly

Laura Merlini<sup>a,\*</sup>, Alessio Bolognesi<sup>b</sup>, Maria Angeles Juanes<sup>a,†</sup>, Franck Vandermoere<sup>c</sup>, Thibault Courtellemont<sup>a,‡</sup>, Roberta Pascolutti<sup>a,§</sup>, Martial Séveno<sup>c</sup>, Yves Barral<sup>b</sup>, and Simonetta Piatti<sup>a</sup>

<sup>a</sup>Centre de Recherche en Biochimie Macromoléculaire, 34293 Montpellier, France; <sup>b</sup>Institute of Biochemistry, ETH Zurich, 8093 Zurich, Switzerland; <sup>c</sup>Functional Proteomic Platform, Institut de Génomique Fonctionnelle, 34094 Montpellier, France

**ABSTRACT** In many cell types, septins assemble into filaments and rings at the neck of cellular appendages and/or at the cleavage furrow to help compartmentalize the plasma membrane and support cytokinesis. How septin ring assembly is coordinated with membrane remodeling and controlled by mechanical stress at these sites is unclear. Through a genetic screen, we uncovered an unanticipated link between the conserved Rho1 GTPase and its effector protein kinase C (Pkc1) with septin ring stability in yeast. Both Rho1 and Pkc1 stabilize the septin ring, at least partly through phosphorylation of the membrane-associated F-BAR protein Syp1, which colocalizes asymmetrically with the septin ring at the bud neck. Syp1 is displaced from the bud neck upon Pkc1-dependent phosphorylation at two serines, thereby affecting the rigidity of the new-forming septin ring. We propose that Rho1 and Pkc1 coordinate septin ring assembly with membrane and cell wall remodeling partly by controlling Syp1 residence at the bud neck.

**Monitoring Editor**  
Francis A. Barr  
University of Oxford

Received: Jun 12, 2015  
Revised: Jul 9, 2015  
Accepted: Jul 10, 2015

## INTRODUCTION

Septins are conserved cytoskeletal proteins that bind and hydrolyze GTP. With the exception of higher plants, they are found in most

eukaryotes, where multiple septins generally assemble into symmetric linear oligomeric complexes. These then polymerize into nonpolar filaments and supramolecular structures such as rings, gauzes, and arcs (reviewed in Beise and Trimble, 2011; Weirich *et al.*, 2008).

This article was published online ahead of print in MBoC in Press (<http://www.molbiolcell.org/cgi/doi/10.1091/mbc.E15-06-0366>) on July 15, 2015.

Present addresses: \*Department of Fundamental Microbiology, University of Lausanne, 1015 Lausanne, Switzerland; †Department of Biology, Rosenstiel Basic Medical Science Research Center, Brandeis University, Waltham, MA 02454; ‡Department of Biochemistry, University of Lausanne, 1066 Epalinges, Switzerland; §Department of Biological Chemistry and Molecular Pharmacology, Harvard Medical School, Boston, MA 02115.

Address correspondence to: Simonetta Piatti ([simonetta.piatti@crbm.cnrs.fr](mailto:simonetta.piatti@crbm.cnrs.fr)).

Abbreviations used: CCD, charge-coupled device; CWI, cell wall integrity; EDTA, ethylenediaminetetraacetic acid; e-GFP, enhanced green fluorescent protein; FACS, fluorescence-activated cell sorter; F-BAR, F-Bin–Amphiphysin–Rvs; 5-FOA, 5-fluoroorotic acid; FRAP, fluorescence recovery after photobleaching; GAP, GTPase-activating protein; GEF, guanine nucleotide exchange factor; GFP, green fluorescent protein; GTP, guanosine triphosphate; MAPK, mitogen-activated protein kinase; MAPKK, mitogen-activated protein kinase kinase; MAPKKK, mitogen-activated protein kinase kinase kinase; MBP, myelin basic protein;  $\mu$ HD, muniscin-homology domain; MS/MS, tandem mass spectroscopy; NP-40, Nonidet-P40; PAK kinase, p21-activated kinase; PBS, phosphate-buffered saline; PI(4,5)P<sub>2</sub>, phosphatidylinositol (4,5)-bisphosphate.

© 2015 Merlini *et al.* This article is distributed by The American Society for Cell Biology under license from the author(s). Two months after publication it is available to the public under an Attribution–Noncommercial–Share Alike 3.0 Unported Creative Commons License (<http://creativecommons.org/licenses/by-nc-sa/3.0/>). “ASCB®,” “The American Society for Cell Biology®,” and “Molecular Biology of the Cell®” are registered trademarks of The American Society for Cell Biology.

Septins are believed to act as cortical organizers by forming lateral diffusion barriers that compartmentalize the plasma membrane into separate domains and shape cellular architectures (reviewed in Barral, 2010; Caudron and Barral, 2009; Mostowy and Cossart, 2012). Septin depletion or mutations disrupt normal morphogenesis and differentiation of sperms, dendrites, and cilia (Hu *et al.*, 2010; Kissel *et al.*, 2005; Tada *et al.*, 2007; Xie *et al.*, 2007; Hu *et al.*, 2010; Kuo *et al.*, 2012) and are linked to a variety of human diseases, such as male sterility, cancer, and neurodegenerative disorders (reviewed in Hall and Russell, 2012; Peterson and Petty, 2010).

In most cases, septins localize to the base of cellular projections, where they demarcate subcellular boundaries. This is the case in the budding yeast *Saccharomyces cerevisiae*, in which septins form a ring at the bud neck—the constriction between mother and future daughter cell (Byers and Goetsch, 1976; Haarer and Pringle, 1987; Kim *et al.*, 1991). In the filamentous fungi *Aspergillus nidulans* and *Ashbya gossypii*, a similar pattern is seen during hyphal branching (Westfall and Momany, 2002; Helfer and Gladfelder, 2006). Furthermore, septins are found at the base of other cellular appendages, such as cilia, dendritic spines, and the flagellum of spermatozoa

(Steels *et al.*, 2007; Tada *et al.*, 2007; Xie *et al.*, 2007; Hu *et al.*, 2010). Thus septin rings are intimately associated with membranes in areas of membrane curvature, which are likely fragile because they are inherently subject to mechanical stress.

Septins associate with membranes through a highly conserved polybasic region at their N-terminus (Zhang *et al.*, 1999; Casamayor and Snyder, 2003). Mammalian septin-4 specifically binds phosphatidylinositol (4,5)-bisphosphate (PI(4,5)P<sub>2</sub>; Zhang *et al.*, 1999). In yeast, PI(4,5)P<sub>2</sub> is enriched in membrane areas of polarized growth and the bud neck (Garrenton *et al.*, 2010) and stimulates formation and organization of septin filaments, which are in turn essential for cell viability (Bertin *et al.*, 2010; McMurray *et al.*, 2011). Indeed, in *S. cerevisiae*, septins are required for cytokinesis by tethering to the division site (i.e., the bud neck) most proteins involved in this process, including components of the contractile actomyosin ring (reviewed in Oh and Bi, 2010; Weirich *et al.*, 2008). Septins are found at the cleavage furrow in fission yeast (Berlin *et al.*, 2003; Tasto *et al.*, 2003), *Caenorhabditis elegans* (Nguyen *et al.*, 2000), *Drosophila* (Neufeld and Rubin, 1994; Fares *et al.*, 1995), and mammalian cells (Kinoshita *et al.*, 1997), suggesting that they contribute to cytokinesis in many organisms.

In migrating cell types such as T-lymphocytes, septins form an annular corset at the cell cortex to rigidify the cell periphery, protect it against mechanical stress, and promote the persistence of migration (Tooley *et al.*, 2009). Thus septins function in a number of mechanical processes at the cell cortex and may therefore respond to mechanical cues. However, the mechanisms driving septin ring assembly at the right positions and in coordination with membrane reorganization are not known. Investigating how fungal septin rings respond to alterations in cell wall organization and the resulting changes in turgor pressure is likely to be very instructive about how septins are regulated in response to mechanical stress.

In fungi, septin localization is dynamic during development and the cell cycle (Caviston *et al.*, 2003; Dobbelaere *et al.*, 2003; Gonzalez-Novo *et al.*, 2008; McMurray and Thorer, 2008; Hernandez-Rodriguez *et al.*, 2012). In budding yeast, septins are first recruited to the presumptive bud site as an unorganized cap, which is rapidly transformed into a cortical septin ring in late G1. At the time of bud emergence, the septin ring expands into an hourglass-like structure referred to as septin collar, which spans the whole bud neck. Immediately before cytokinesis, the collar splits into two distinct rings that sandwich the contractile ring (reviewed in Oh and Bi, 2010; Weirich *et al.*, 2008). Fluorescence recovery after photobleaching (FRAP) experiments indicate that septin structures are highly dynamic before bud emergence. On bud emergence, the septin collar at the bud neck is conversely very rigid, whereas at cytokinesis the split septin rings become dynamic again (Caviston *et al.*, 2003; Dobbelaere *et al.*, 2003). In mammalian cells, septin rings remain dynamic throughout cytokinesis, rapidly exchanging septin subunits with the cytoplasm (Schmidt and Nichols, 2004). The dynamics of mammalian septins at other submembrane ring structures is not known.

In budding yeast, the Cdc42 GTPase of the Rho family plays a crucial role in the recruitment of septins to the presumptive bud site (Cid *et al.*, 2001; Iwase *et al.*, 2006), and cycles of Cdc42 GTP binding and hydrolysis are required for septin collar formation (Gladfelter *et al.*, 2002; Caviston *et al.*, 2003). Polarized exocytosis sculpts the septin ring by driving the insertion of membrane into the emerging bud, thereby hollowing the septin cap into a ring (Okada *et al.*, 2013). Several protein kinases, such as Cla4, Gin4, and Elm1, as well as septin-interacting proteins, such as Bni5, locate to the bud neck in a septin-dependent manner and promote septin collar stabilization (Longtine *et al.*, 1998; Barral *et al.*, 1999; Lee *et al.*, 2002). Finally, the protein phosphatase PP2A bound to its B' regulatory subunit, Rts1,

promotes timely septin disassembly after cytokinesis (Dobbelaere and Barral, 2004). How these regulators directly or indirectly promote septin ring assembly and disassembly at the bud neck is not clear.

A key question is how septin dynamics is coupled to the dramatic membrane rearrangements occurring during the formation of cellular protrusions. We set out to address this question using budding yeast as model system. We took advantage of our previous finding that the ubiquitin ligases Dma1 and Dma2 are essential together with the PAK kinase Cla4 for septin ring formation and stabilization. Indeed, *dma1 dma2 cla4* triple mutants show pronounced septin localization defects and cytokinesis failure and are unviable (Fraschini *et al.*, 2004; Merlini *et al.*, 2012). We used this observation to set up a genetic screen aiming at the identification of novel regulators of septin dynamics. Here we report for the first time that the conserved Rho1 GTPase, its target protein kinase C, and the F-BAR protein Syp1 that induces membrane curvature promote robust septin recruitment and likely coordinate membrane and septin reorganization during budding.

## RESULTS

### A genetic screen for novel regulators of septin dynamics identifies the Rho1 GTPase and its target, Pkc1

Because *dma1 dma2 cla4* triple-mutant cells are not viable and show strong septin organization defects (Fraschini *et al.*, 2004; Merlini *et al.*, 2012), we wondered whether the lack of viability of these cells was mainly due to the collapse of septin structures. We rationalized that if this were the case, extragenic suppressors of the lethality of *dma1 dma2 cla4* cells would most likely identify regulators of septin dynamics (see *Materials and Methods*). To test this possibility and identify new regulators of septin dynamics, we isolated 44 independent suppressors that restored cell viability in the total absence of *DMA1*, *DMA2*, and *CLA4*. Genetic tests classified 11 of the suppressing mutations as dominant, 10 as semidominant, and 19 as recessive. Four suppressors were sterile, hampering the assessment of their dominance/recessivity. FACS analysis of DNA contents showed that several suppressors completed cytokinesis properly (unpublished data), supporting the idea that septin organization was restored. We subsequently focused our attention on one of the best dominant suppressors of the temperature sensitivity of *dma1Δ dma2Δ cla4-75* triple-mutant cells (Figure 1A). This suppressor indeed restored septin ring assembly and position at the bud neck, as determined using the septin Shs1 fused to green fluorescent protein (GFP) as reporter and demonstrated by the fact that it restored cytokinesis in the complete absence of *DMA1*, *DMA2*, and *CLA4* (Figure 1E and Supplemental Figure S1B). Thus, restoring septin organization appeared to rescue the lethality of the *dma1 dma2 cla4* triple mutant. We concluded that our suppressors might indeed identify new regulatory pathways of septin function.

The foregoing strong suppressor mutation mapped in the *RHO1* gene, which encodes the yeast counterpart of the conserved GTPase RhoA (Qadota *et al.*, 1994). In metazoans, RhoA is required for cytokinesis through assembly and contraction of the contractile actomyosin ring (reviewed in Glotzer, 2005; Pollard and Wu, 2010; Green *et al.*, 2012). The suppressor mutation was due to a single nucleotide substitution replacing the aspartic acid in position 72, which is located inside the highly conserved switch II of the guanine nucleotide-binding domain of Rho GTPases (Figure 1B), by asparagine (*RHO1-D72N*). This finding prompted us to sequence *RHO1* in all the other dominant suppressors. Strikingly, three additional suppressors carried exactly the same *RHO1-D72N* mutation (unpublished data).

The *RHO1-D72N* allele likely causes Rho1 hyperactivation, at least toward some of its effectors. Indeed, similar to *RHO1-D72N*,

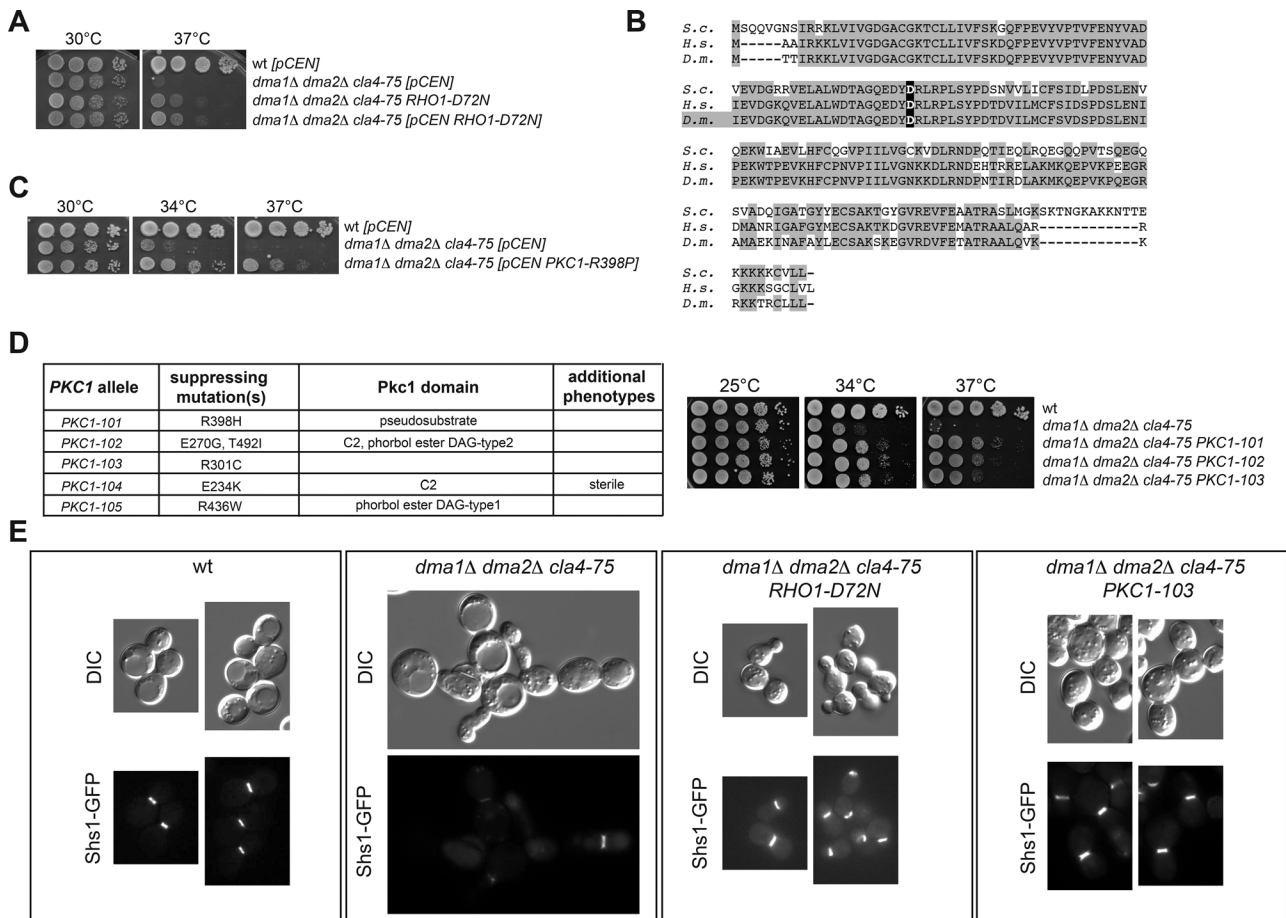


**FIGURE 1:** Rho1 and Pkc1 hyperactivation suppresses the temperature sensitivity of *dma1Δ dma2Δ cla4-75* cells. (A, C, D) Serial dilutions of strains with the indicated genotypes were spotted on YEPD plates and incubated at the indicated temperatures for 2 d. The table in D lists the *PKC1* alleles isolated in our genetic screen as suppressors of the lethality of *dma1Δ dma2Δ cla4Δ* cells. (B) Amino acid sequence alignment of Rho1/RhoA from budding yeast (*S.c.*), human (*H.s.*), and fruit fly (*D.m.*). The aspartate in bold is the conserved residue changed to asparagine in the *RHO1-D72N* allele. (E) Representative images of cells with the indicated genotypes and expressing Shs1-GFP after shift to 37°C for 6 h.

an episomal plasmid bearing the GTP-locked *RHO1-G19V* allele, but not the dominant-negative *RHO1-D125A* allele, suppressed the temperature sensitivity of *dma1Δ dma2Δ cla4-75* triple-mutant cells (Supplemental Figure S1C). Furthermore, deletion of *LRG1* and *SAC7*, which encode the main GTPase-activating proteins (GAPs) for Rho1 down-regulation during cytokinesis (Yoshida *et al.*, 2009), partially suppressed the lethality of *dma1Δ dma2Δ cla4-75* cells at high temperatures (Supplemental Figure S1D). In addition, we found that one of the recessive suppressors isolated in our genetic screen carried a premature stop codon in *LRG1* (*LRG1-L67stop*). Conversely, eliminating the *Sac7* paralogue *Bag7* (Supplemental Figure S1D) or mutating the catalytic residue of the Rho GAP *Bem2* (Marquitz *et al.*, 2002; unpublished data) did not rescue the temperature sensitivity of *dma1 dma2 cla4-75* triple-mutant cells. Finally, since the yeast polo-like kinase, encoded by the *CDC5* gene, recruits and activates Rho1 at the cell division site for cytokinesis (Yoshida *et al.*, 2006), we asked whether the *RHO1-D72N* allele could partially rescue the temperature-sensitive growth defects of *cdc5* mutants. This was indeed the case (Supplemental Figure S1E), suggesting that the *Rho1-D72N* protein is likely hyperactive.

The *RHO1-D72N* allele also partially suppressed the temperature sensitivity of septin mutants like *cdc12-1*, which fails to assem-

ble the septin ring, *cdc12-6*, which disassembles the septin ring upon shift to the restrictive temperature (Barral *et al.*, 2000; Dobbelaere *et al.*, 2003), and *shs1Δ*, which lacks the only nonessential septin (Figure 2, A–C, and Supplemental Figure S2, A and B), suggesting that septin stabilization may underlie the mechanism of suppression. This conclusion was confirmed by direct inspection of the septin ring marked by GFP-Cdc3 in *cdc12-6* cells shifted to the nonpermissive temperature of 30°C. Whereas *cdc12-6* cells, either cycling (Figure 2, B and C) or arrested in mitosis by nocodazole treatment (Figure 2, D and E), rapidly disassembled the septin ring after 1-h shift to 30°C, a significant fraction of them could maintain a septin ring at the bud neck upon expression of *RHO1-D72N*.

Although constitutively active GTP-locked variants of Rho1 as sole source of Rho1 in the cell cannot support actomyosin ring assembly and viability of yeast cells (Yoshida *et al.*, 2009), *RHO1-D72N* cells were perfectly viable, assembled a normal actomyosin ring and contracted it with kinetics similar to that of wild-type cells (Supplemental Figure S3). Thus *Rho1-D72N* might be hyperactive toward some but not all Rho1 effectors.

Because the Rho GTPase *Cdc42* is known to promote septin deposition (Gladfelter *et al.*, 2002; Caviston *et al.*, 2003), we tested whether the hyperactive *CDC42-D65N* allele (Mosch *et al.*, 2001),

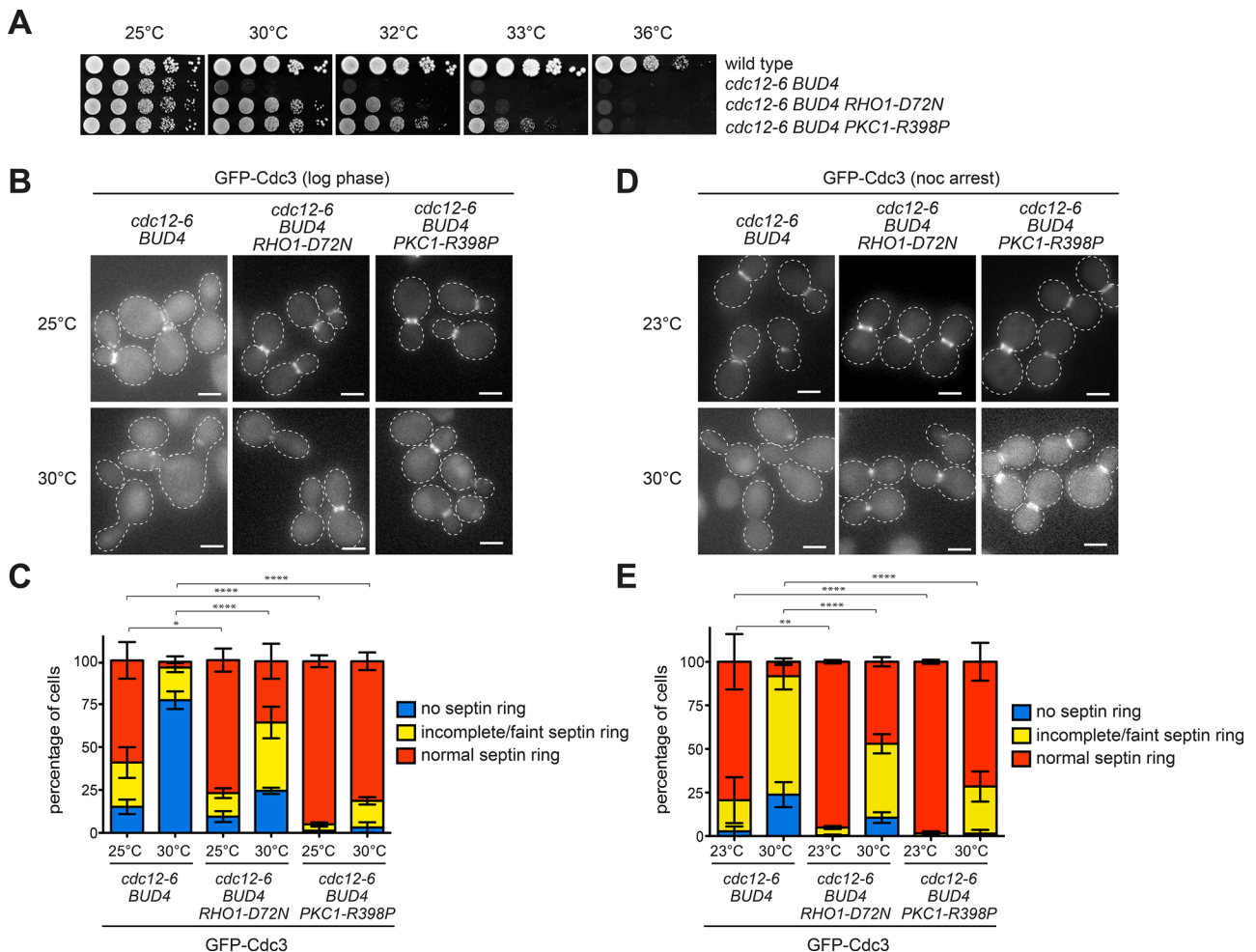


**FIGURE 2:** Rho1 and Pkc1 hyperactivation rescues the septin ring instability of *cdc12-6* mutant cells. (A) Serial dilutions of strains with the indicated genotypes were spotted on YEPD plates and incubated at the indicated temperatures for 2 d. (B, C) *cdc12-6 BUD4*<sup>+</sup> cells expressing wild-type *RHO1* and *PKC1*, *RHO1-D72N*, or *PKC1-R398P* at their respective genomic loci were grown at 25°C and shifted to the restrictive temperature of 30°C for 1 h. The septin ring is marked by GFP-Cdc3. Average values and error bars (SD) are derived from three independent experiments ( $n \geq 100$ ). (D, E) The same strains as in B and C were grown at 23°C, arrested in mitosis by 3 h of treatment with nocodazole, and shifted to 30°C for 1 h to image GFP-Cdc3. Average values and error bars (SD) are derived from three independent experiments ( $n \geq 100$ ). Scale bars, 5  $\mu$ m.

which carries a synonymic mutation to *RHO1-D72N*, could suppress the temperature sensitivity of *dma1 dma2 cla4-75* triple-mutant or *cdc12* single-mutant cells. Expression of *CDC42-D65N* had no effect on cell division of *dma1 dma2 cla4-75* triple-mutant and *cdc12-6* single-mutant cells, whereas it was detrimental for *cdc12-1* cells growing at the permissive temperature (Supplemental Figure S2, D–F). Consistent with these data, GTP-locked Cdc42 negatively regulates septin polymerization in budding yeast (Gladfelter et al., 2002) and mammalian cells (Joberty et al., 2001).

Five Rho1 effectors are known: protein kinase C (Pkc1), the formins Bni1 and Bnr1, the exocyst component Sec3, and the Fks1/2 glucan synthase (Levin, 2011). Pkc1 is a major regulator of membrane dynamics (Kono et al., 2012) and localizes, like Rho1, to sites of polarized growth and the bud neck (Yamochi et al., 1994; Denis and Cyert, 2005). Furthermore, it is the only bud neck protein that colocalizes with septins also in meiosis (Lam et al., 2014), which makes it an excellent Rho1-target candidate in the regulation of septin stability. Consistently, the *PKC1-R398P* hyperactive allele, which is mutated in the pseudosubstrate autoinhibitory domain (Nonaka et al., 1995),

suppressed the temperature sensitivity of *dma1Δ dma2Δ cla4-75* triple-mutant (Figure 1C) and *cdc12-1* and *cdc12-6* single-mutant cells (Figure 2A and Supplemental Figure S2C). This was not the case for a dominant hyperactive allele of *BNI1* (*BNI1-V360D*; Kono et al., 2012; unpublished data). Furthermore, *PKC1-R398P* efficiently suppressed septin ring disassembly of *cdc12-6* cells at restrictive temperature (Figure 2, B–E). Finally, direct sequencing showed that five dominant suppressors found in our genetic screen carried *PKC1* mutations in different protein domains (*PKC1-R398H*, *PKC1-E270G*, *T492I*, *PKC1-R301C*, *PKC1-E234K*, and *PKC1-R436W*; Figure 1, D and E), further corroborating the idea that hyperactivation of the Rho1/Pkc1 pathway stabilizes the septin ring.

### Rho1 and Pkc1 stabilize the septin ring

Although the involvement of Rho1/RhoA in the assembly and contraction of the actomyosin ring is well established, no data linked its function to septins. We therefore tested directly the effect of Rho1 and Pkc1 on septin dynamics. The septin ring was visualized by expression of GFP-Cdc12 and its stability analyzed by FRAP. As

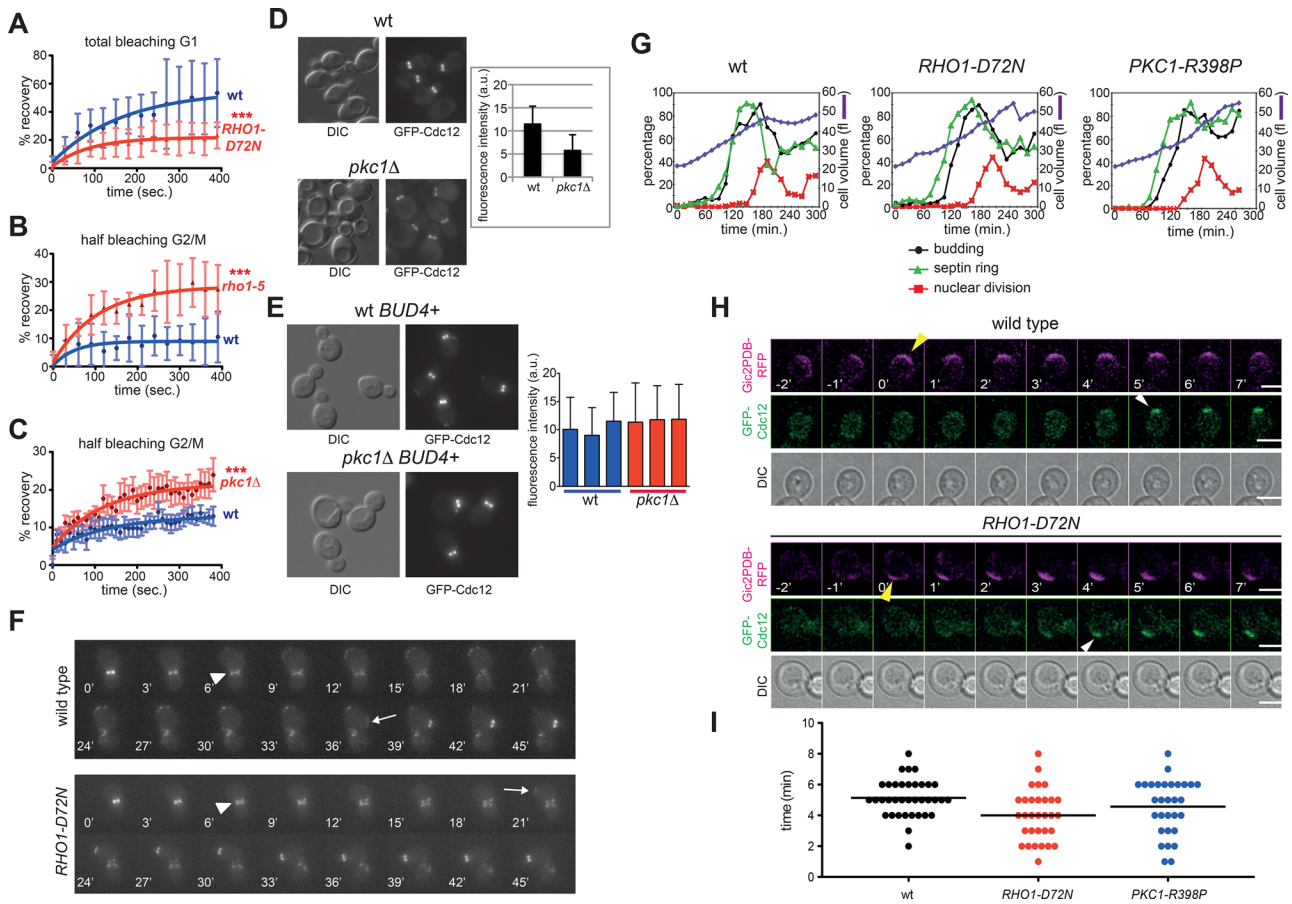


**FIGURE 3: *RHO1* and *PKC1* mutations affect septin dynamics.** (A) FRAP analysis of the septin ring in G1 cells after complete bleaching of the GFP-Cdc12 fluorescence signal at the presumptive bud site (time 0: postbleach). (B, C) FRAP analysis of the septin ring in budded cells after bleaching of half of the GFP-Cdc12 fluorescence signal at the bud neck (time 0: postbleach). Curves were fitted to monoexponential decay. (D) Wild-type and *pkc1Δ* cells in the W303 background (*bud4*) were grown in sorbitol-containing YEPD medium at 30°C and imaged. Fluorescence intensities of GFP-Cdc12 signals at the bud neck were quantified on one single in-focus plane ( $n \geq 100$ ). (E) Three independent wild-type and *pkc1Δ* strains in W303 carrying a wild-type copy of *BUD4* (*BUD4*<sup>+</sup>) were grown and imaged as in D to quantify fluorescence intensities of GFP-Cdc12 signals at the bud neck ( $n \geq 100$ ). (F) Representative movies of wild-type and *RHO1-D72N* cells expressing GFP-Cdc12. Arrowheads indicate splitting of the septin ring, whereas arrows indicate appearance of a new septin ring. Time 0 is arbitrarily set 6 min before septin ring splitting. (G) Small, unbudded cells of wild-type, *RHO1-D72N*, and *PKC1-R398P* cells were isolated by centrifugal elutriation and released in fresh YEPD medium at 25°C (time 0). At the indicated time points, cells were collected for FACS analysis of DNA contents (not shown) and kinetics of cell volume, budding, nuclear division, and septin ring formation. This last was analyzed by indirect immunofluorescence with anti-Cdc11 antibodies. (H, I) Wild-type, *RHO1-D72N*, and *PKC1-R398P* cells expressing GFP-Cdc12 and the Gic2PDB-RFP marker of Cdc42 activation were filmed at 30°C to measure the time interval between Cdc42 activation and septin recruitment. The graph (I) represents the distribution of time intervals in each strain ( $n \geq 30$ ) and mean times (black bars).

expected (Caviston *et al.*, 2003; Dobbelaere *et al.*, 2003), after its complete bleaching in late G1, there was efficient fluorescence recovery in wild-type cells (Figure 3A), indicating high turnover of septins at the presumptive bud site (mobile fraction  $54 \pm 21\%$ ,  $n = 10$ ). In contrast, turnover was lower in *RHO1-D72N* cells (mobile fraction  $25 \pm 11\%$ ,  $n = 10$ ), indicating that in these cells the septin ring exchanged less rapidly with the cytoplasmic pool and was more rigid already in G1. We then asked whether *RHO1* inactivation destabilizes the septin ring. To this end, we used the temperature-sensitive *rho1-5* mutant, which is most likely specifically defective in Pkc1 activation since its temperature sensitivity is efficiently suppressed by *PKC1* overexpression (Kamada *et al.*, 1996) and the *PKC1-R398P* allele (unpublished data). Half of the GFP-Cdc12 signal

was bleached in large-budded cells. Consistent with the frozen state of the ring at this cell cycle stage (Caviston *et al.*, 2003; Dobbelaere *et al.*, 2003), turnover at 37°C was low in wild-type cells (mobile fraction  $10 \pm 6\%$ ,  $n = 12$ ). In contrast, recovery was significantly higher in *rho1-5* cells at 37°C (Figure 3B; mobile fraction  $31 \pm 9\%$ ,  $n = 7$ ), indicating that Rho1 inactivation enhances septin ring turnover.

Because the *PKC1* gene is essential for viability and cell integrity, to test its possible involvement in septin dynamics, we had to grow *pkc1Δ* cells in the presence of an osmostabilizer (i.e., sorbitol). Under these growth conditions, *PKC1* deletion accelerated the turnover of GFP-Cdc12 at the septin ring in budded cells (Figure 3C; mobile fraction  $11.5 \pm 6.5\%$ ,  $n = 8$ , for wild-type and  $22 \pm 8\%$ ,  $n = 8$ , for *pkc1Δ* cells). Thus inactivation of Rho1 and Pkc1 increases the

fluidity of the septin ring, whereas *RHO1* hyperactivation makes the septin ring more rigid. In agreement with this conclusion, even when incubated at 25°C and provided with sorbitol, combining *PKC1* deletion with the *cdc12-1* or *cdc12-6* temperature-sensitive mutations dramatically compromised viability (unpublished data), whereas *pkc1Δ shs1Δ* double-mutant cells were inviable. These data indicate that Pkc1 becomes essential in the presence of septin defects that are normally tolerated by otherwise wild-type cells.

Mutants affecting Rho1 activity were previously shown to assemble septin rings but fail to undergo the normal conversion from single ring into hourglass (Cid et al., 2001). Similarly, we found that *PKC1* deletion in the W303 strain background led to thinner septin rings containing lower amounts of GFP-Cdc12 than otherwise wild-type cells (Figure 3D). Because W303 bears a frameshift mutation in the *BUD4* gene (Voth et al., 2005), which encodes an anillin-related protein that stabilizes the septin ring during splitting (Wloka et al., 2011; Kang et al., 2013), we asked whether introduction of a wild-type copy of *BUD4* restored normal septin levels at the bud neck of *pkc1Δ* cells. This was indeed the case (Figure 3E), suggesting that Pkc1 and Bud4 play overlapping role(s) in septin ring stability during a normal cell cycle.

In agreement with the idea that Rho1 and Pkc1 stabilize the septin ring, we found that their hyperactivation shortened the interval between septin ring splitting and formation of a new septin ring—that is, the cell cycle window characterized by the highest septin dynamics. Time-lapse video microscopy of wild-type and *RHO1-D72N* cells expressing GFP-Cdc12 showed that the time between septin ring splitting and formation of a new septin ring was on average  $21 \pm 6.9$  min in *RHO1-D72N* cells ( $n = 100$ ) and  $34 \pm 11.5$  min in wild-type cells ( $n = 72$ ; Figure 3F). To confirm these results, we elutriated small, unbudded cells from wild-type, *RHO1-D72N* and *PKC1-R398P* cell cultures and released them in fresh medium at 25°C. At various times, cell samples were collected, and cell volume (used as internal reference), budding, septin ring formation, and nuclear division were quantified. In all three strains, bud emergence occurred at the same mean cell volume (34 fl), suggesting that this process is not grossly affected by *RHO1* and *PKC1* hyperactivation. Under these conditions, wild-type cells formed septin assemblies concomitant to budding and S-phase entry (starting at 90 min after release). In contrast, in the *RHO1-D72N* and *PKC1-R398P* mutant cells, septin ring recruitment took place at a smaller cell volume and was advanced by ~15 min relative to budding and S-phase entry (Figure 3G). Of importance, in these mutants septin deposition still occurred after activation of Cdc42, as shown by time-lapse video microscopy of cells expressing the fluorescent Cdc42 biosensor Gic2PBD–red fluorescent protein (Okada et al., 2013; Figure 3H). However, the time interval between Cdc42 activation and septin recruitment was slightly shorter in the mutants relative to wild-type cells (Figure 3I).

Collectively these data indicate that Rho1 and Pkc1 contribute to septin ring stabilization.

### Osmotic stabilization of the cell wall restores septin organization in a septin mutant

Rho1 and Pkc1 are involved in the cell wall integrity (CWI) pathway, which responds to a variety of cell wall stresses (e.g., osmotic stress) and activates a mitogen-activated protein kinase (MAPK) cascade response. This in turn induces a specific transcriptional program regulating the expression of cell wall enzymes and reorganization of the actin cytoskeleton (Levin, 2011; Supplemental Figure S4A). We therefore asked whether osmotic support, through addition of sorbitol to the growth medium, might also promote

septin ring stabilization by counteracting the intracellular turgor pressure. The temperature sensitivity of *cdc12-1* and *cdc12-6* cells was indeed partially suppressed by sorbitol (Figure 4A). To investigate whether sorbitol could also stabilize the septin ring of *cdc12-1* cells, we grew wild-type and *cdc12-1* cells at 23°C, arrested them in G1, and released them at 34°C in rich medium either lacking or containing sorbitol. FACS analysis of DNA contents at different time points after release showed that in the absence of sorbitol, *cdc12-1* cells displayed pronounced cytokinetic defects leading to polyploidy, which were efficiently rescued by sorbitol (Figure 4B). Strikingly, whereas in the absence of sorbitol septin rings failed to assemble in most *cdc12-1* cells, in the presence of sorbitol they assembled at the bud neck in a high fraction of them with kinetics similar to wild type (Figure 4, C and D). Furthermore, sorbitol efficiently rescued also the elongated-bud phenotype of *cdc12-1* cells at 34°C (Figure 4E). Thus, similar to hyperactivation of the Rho1/Pkc1 pathway, counteracting osmotic stress may stabilize the septin ring.

### Rho1 and Pkc1 likely have targets other than the cell wall integrity pathway in septin stabilization

Because Rho1 and Pkc1 are involved in the CWI pathway (Supplemental Figure S4A), we wondered whether hyperactivation of the MAPK cascade downstream of Pkc1 was involved in the suppression of the lethality of *dma1 dma2 cla4* triple-mutant cells by *RHO1* and *PKC1* dominant alleles. Whereas hyperactivation of the most upstream MAPKKK in this pathway, using the *BCK1-20* allele, weakly suppressed the temperature sensitivity of *dma1Δ dma2Δ cla4-75* triple-mutant cells, hyperactivation of the downstream MAPKK and MAPK by the dominant *MKK1-S386P* or overexpression of Slt2 (Irie et al., 1993) did not (Supplemental Figure S4B). Thus Rho1- and Pkc1-mediated suppression of the septin defects caused by simultaneous inactivation of Dma1, Dma2, and Cla4 is not caused solely by hyperinactivation of the MAPK pathway, if at all. Consistently, the *RHO1-D72N* allele that we isolated in our genetic screen did not hyperactivate the MAPK cascade after thermal stress, as judged by phosphorylation of the MAPK Slt2 (Supplemental Figure S4C). Although our data do not rule out a possible contribution of the CWI pathway on septin ring stability, they do suggest that Rho1 and Pkc1 stabilize the septin ring at least partly independently of the MAP kinase pathway.

### The F-BAR protein Syp1 is a novel Pkc1 phosphorylation target

High-throughput analysis of the budding yeast kinome revealed a physical interaction between Pkc1 and Syp1 (Breitkreutz et al., 2010), a membrane protein of the F-BAR family that has been implicated in endocytosis and septin dynamics at the bud neck (Boettner et al., 2009; Reider et al., 2009; Stimpson et al., 2009). *SYP1* deletion partially suppressed the temperature sensitivity of *cdc12-1* and *dma1Δ dma2Δ cla4-75* triple-mutant cells (Supplemental Figure S5A), suggesting that it might be a relevant target of Pkc1 in septin regulation.

*PKC1* inactivation severely compromised the organization of Syp1 in patches while enhancing its bud neck localization (Figure 5A), suggesting that Pkc1 controls the turnover of Syp1 at membranes and its displacement from the bud neck. To gain insights into the relationship between the bud neck localization of Syp1 and that of septins, we first analyzed the localization of Syp1–enhanced GFP (eGFP) during the cell cycle, starting from cells synchronized in G1 by  $\alpha$ -factor and released in fresh medium at 25°C. Consistent with published data (Qiu et al., 2008; Reider et al.,

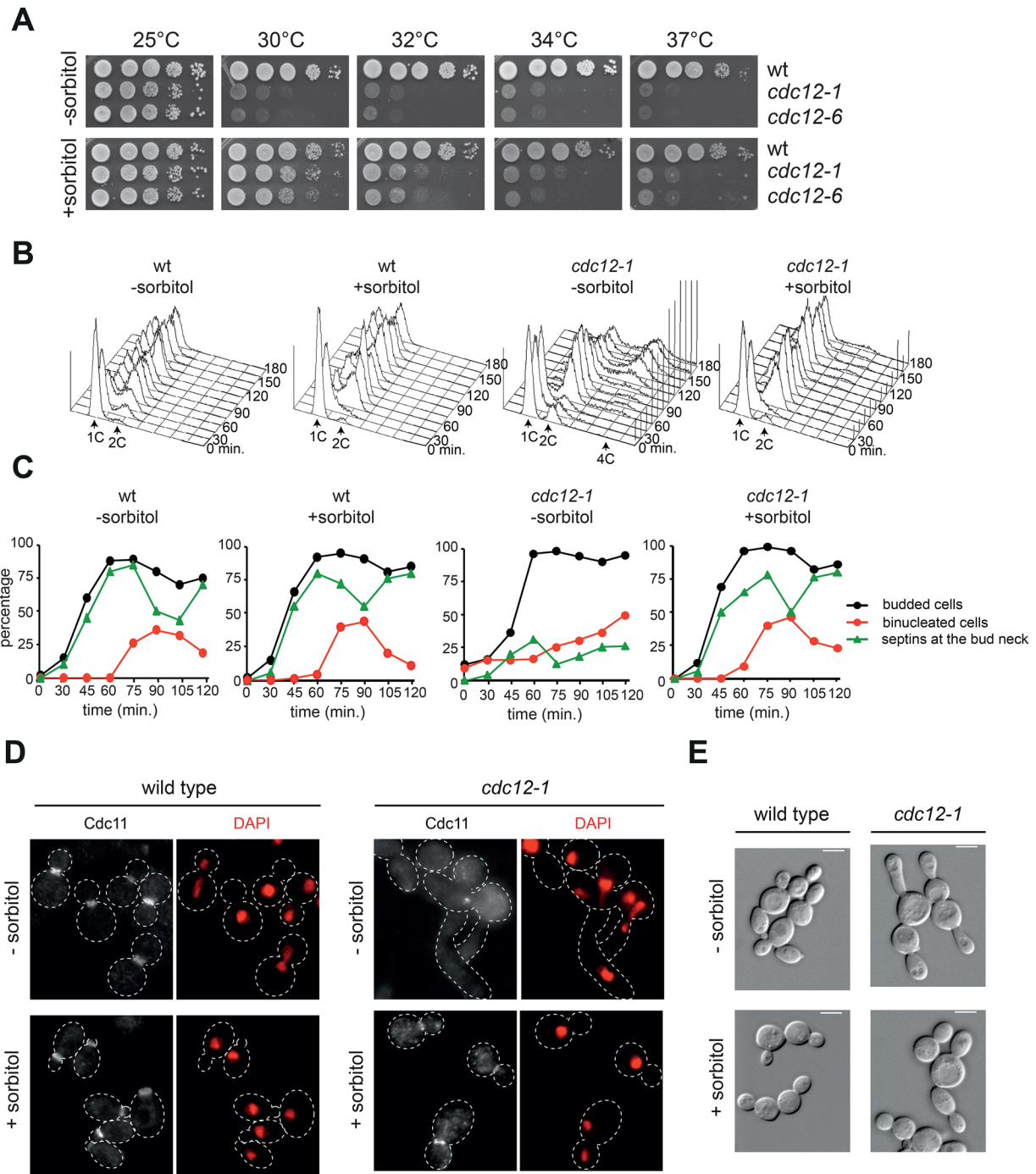
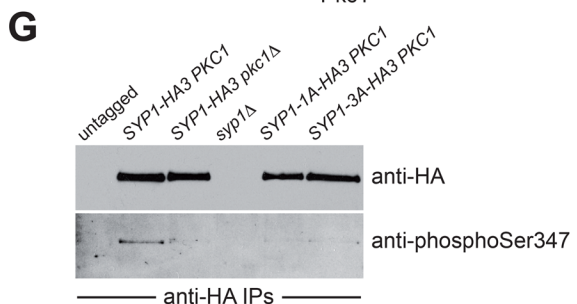
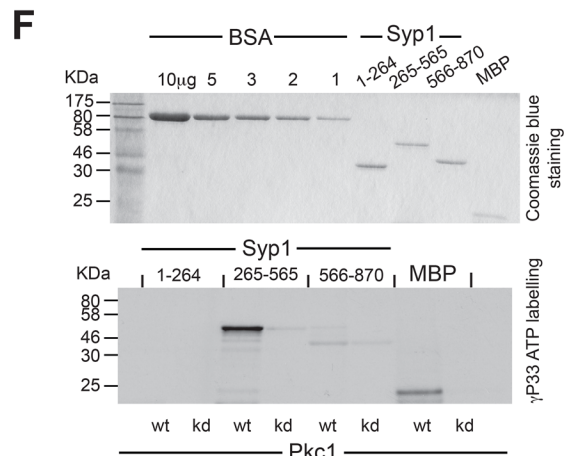
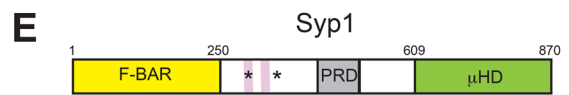
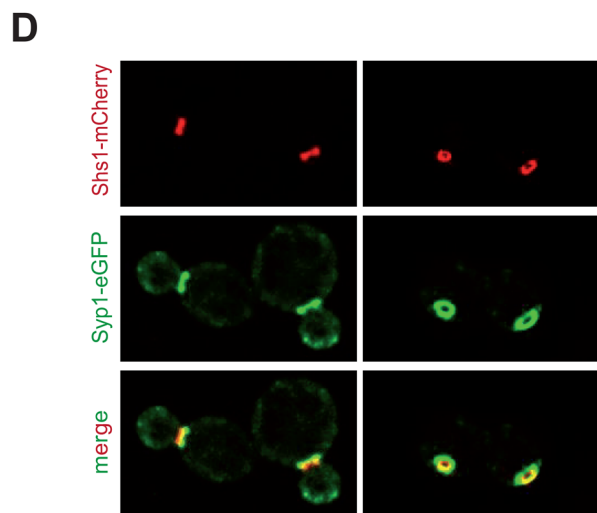
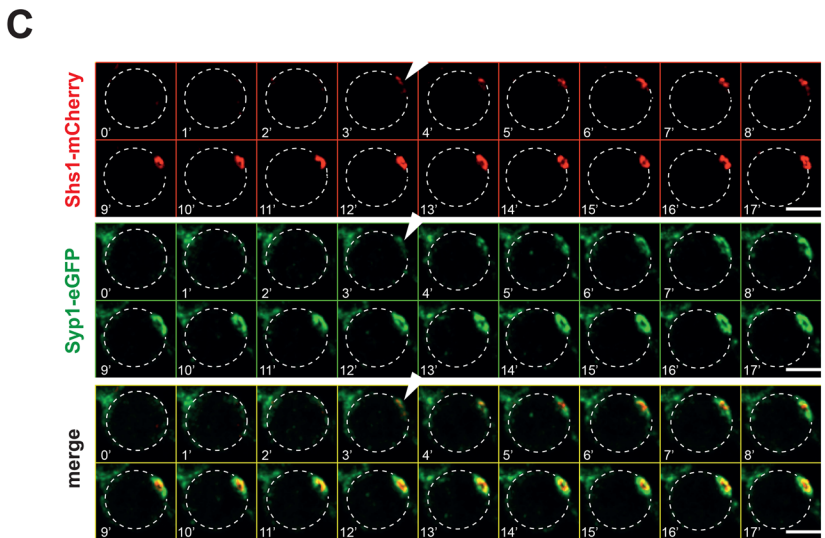
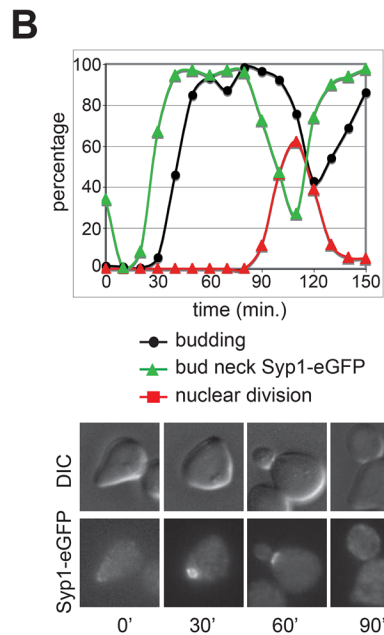
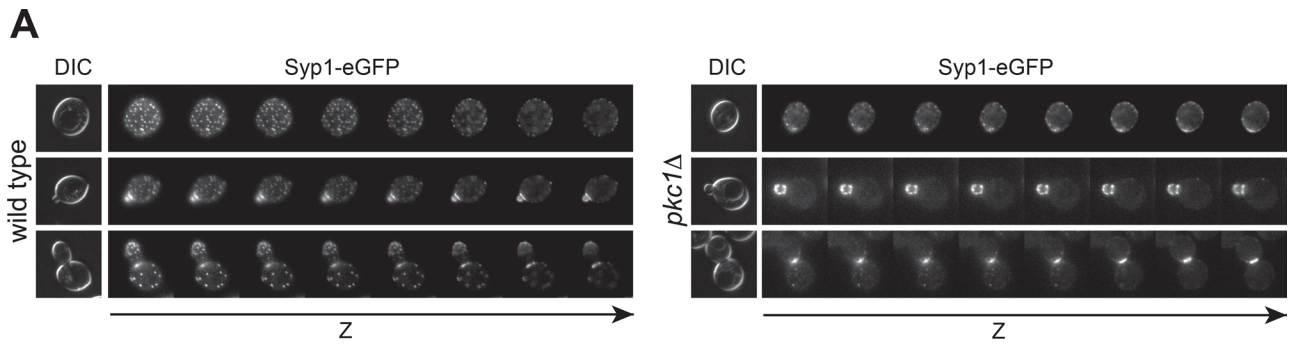


**FIGURE 4:** Hyperosmotic medium rescues the lethality and cytokinetic defects of septin mutants. (A) Serial dilutions of strains with the indicated genotypes were spotted on YEPD plates and incubated at the indicated temperatures for 2 d. (B–E) Wild-type and *cdc12-1* cells were grown in YEPD at 25°C in the absence or presence of sorbitol, arrested in G1 by  $\alpha$ -factor, and released in fresh medium at 34°C (time 0). At the indicated time points, cell samples were collected for FACS analysis of DNA contents (B) and kinetics of budding, nuclear division, and septin deposition at the bud neck by indirect immunofluorescence of the septin Cdc11 (C). Distribution of septins (D) and cell morphology (E) in representative cells at  $t = 120$  min after release.

2009), Syp1-eGFP was recruited to the bud neck in late G1, before bud emergence. Its levels then decreased at the bud neck around the time of anaphase entry, marked by the increase in binucleate cells (Figure 5B). Time-lapse video microscopy of cells expressing at the same time Syp1-eGFP and Shs1-mCherry revealed that Syp1 was recruited to the bud neck concomitant to

septins (Figure 5C). Syp1 rings were larger than septin rings and asymmetrically localized to the mother side of the bud neck in small/medium-budded cells (Figure 5D), similar to the phosphatase complex Bni4/Glc7 (DeMarini *et al.*, 1997; Kozubowski *et al.*, 2003) and the SUMO E3 ligases Siz1 and Siz2 (Johnson and Blobel, 1999; Johnson and Gupta, 2001). Deletion of *PKC1* or



*DMA1* and *DMA2* did not appear to affect the pattern of Syp1 localization at the bud neck during the cell cycle (Supplemental Figure S5, B and C).

We then asked whether Syp1 could be phosphorylated by Pkc1. Syp1 carries an N-terminal F-BAR domain, followed by a central, unstructured region and a C-terminal  $\mu$ HD domain that interacts with the endocytic protein Ede1 and the Rho1 activator Mid2. In addition, the region spanning amino acids 265–365 carries a liposome-binding domain and two lysine-rich motifs that bind PI(4,5)P<sub>2</sub> and contribute to Syp1 association with the plasma membrane (Reider *et al.*, 2009; Figure 5E). We purified from bacterial cells the N-terminal (amino acids [aa] 1–265), the central (aa 265–565), and the C-terminal (aa 566–870) domains of Syp1 and subjected them to *in vitro* kinase assays using wild-type or kinase-dead Pkc1 immunoprecipitated from yeast cell extracts, using myelin basic protein (MBP) as control substrate (Antonsson *et al.*, 1994). As shown in Figure 5F, Pkc1, but not its kinase-dead version, efficiently phosphorylated the central region of Syp1, as well as MBP. Mass spectrometric analysis of this truncated protein identified two Pkc1-dependent phosphorylation sites on Ser-347 and Ser-389 or Ser-390 (Supplemental Table S1). Both are located in proximity of the two lysine-rich motifs (Figure 5E) and are hence likely to regulate Syp1 interaction with membranes. These phosphosites were previously mapped *in vivo*, along with many additional phosphorylation sites (Li *et al.*, 2007; Albuquerque *et al.*, 2008; Holt *et al.*, 2009; Bodenmiller *et al.*, 2010; Breitzkreutz *et al.*, 2010). Of interest, phosphorylation of Ser-347 was found to increase in response to osmotic stress (Soufi *et al.*, 2009) and rapidly decrease in sorbitol-containing medium (Kanshin *et al.*, 2015). In spite of that, using antibodies specific for phosphorylated Ser-347, we could detect low levels of Syp1 Ser-347 phosphorylation in wild-type but not in *pkc1Δ* cells grown in sorbitol-containing medium (Figure 5G), suggesting that Syp1 is a substrate of Pkc1 also *in vivo*. Thus Pkc1 phosphorylates Syp1 directly on Ser-347 and probably Ser-389/Ser-390 *in vitro* and *in vivo* and regulates its subcellular localization. Syp1 is the second bona fide substrate of Pkc1 in budding yeast, the first being Bck1 (Levin *et al.*, 1994).

### Syp1 phosphorylation by Pkc1 increases its turnover at the bud neck and contributes to the robustness of septin deposition

Pkc1-dependent phosphorylation of the central region of Syp1 would introduce negative charges in an otherwise basic domain,

which could interfere with Syp1 interaction with membranes. Consistently, in *pkc1Δ* mutant cells Syp1 localization at the bud neck increased compared with wild-type cells at the cost of patches normally observed at the rest of the cortex (Figure 5A). These data suggest that Pkc1 inactivation stabilizes Syp1 at the bud neck. To address the physiological role of the Pkc1-dependent phosphorylation sites, we mutated Ser-347, Ser-389, and Ser-390 to alanine to abolish phosphorylation and to aspartate to mimic constitutive phosphorylation. The mutant alleles were then integrated in the yeast genome as the only copy of *SYP1* in the cells and will be referred to as *SYP1-3A* and *SYP1-3D*, respectively. The corresponding mutant proteins tagged with eGFP were expressed at levels similar to those of their wild-type counterpart (Figure 6A) and recruited to the bud neck with the same timing during the cell cycle (unpublished data). We then assessed by FRAP whether they affected Syp1 turnover at the bud neck (Figure 6B). On bleaching of half of the Syp1-eGFP ring in small/medium-budded cells, ~39% of the molecules recovered (mobile fraction), with a half-recovery time of  $13.63 \pm 0.59$  s. A similar mobile fraction was observed for Syp1-3D-eGFP, but its half-recovery time decreased to  $6.77 \pm 0.77$  s, indicating a faster turnover. In stark contrast, the mobile fraction of Syp1-3A-eGFP was reduced to 18% (half-recovery time of  $10.79 \pm 0.5$  s), indicating that the protein is more stably bound to the cortex. Therefore, Pkc1-dependent phosphorylation stimulates the turnover of Syp1 at the bud neck, consistent with the effect of *PKC1* inactivation on Syp1 localization.

We then assessed the effects of *SYP1* phosphomutant alleles on septin dynamics by analyzing by FRAP the recovery rates of GFP-Cdc12 at the bud neck. Recovery of GFP-Cdc12 after bleaching of the entire septin ring is indicative of septin recruitment from the cytoplasm, whereas recovery after half-bleaching of the ring is the result of both lateral diffusion from the unbleached half and septin recruitment from the cytoplasm. We measured recovery of GFP-Cdc12 in wild-type *SYP1*, *syp1Δ*, *SYP1-3A*, and *SYP1-3D* cells in late G1 after bleaching of both entire and half septin rings (Figure 6, C and D). To assess specifically the internal fluidity of the septin ring and have a more precise measurement of the lateral diffusion only, we subtracted the averaged values of recovery upon entire bleaching from those obtained after half-bleaching. Strikingly, the septin ring was significantly more rigid in *syp1Δ* and *SYP1-3D* cells than in wild-type and *SYP1-3A* cells (Figure 6E), suggesting that Pkc1-dependent phosphorylation and removal of Syp1 stabilizes the septin ring in late G1. Hence Syp1 localization to the bud neck in G1

**FIGURE 5:** Pkc1 phosphorylates Syp1 and controls its bud neck localization. (A) Z-stack serial images of wild-type and *pkc1Δ* cells expressing Syp1-eGFP at different cell cycle stages (top: G1, unbudded; middle: S phase, small budded; bottom: mitosis, large budded). Spacing between sequential planes is 0.3  $\mu$ m. (B) Wild-type cells expressing Syp1-eGFP were arrested in G1 by  $\alpha$ -factor and released in fresh YEPD medium at 25°C. At the indicated time points, cells were collected for FACS analysis of DNA contents (not shown) and kinetics of budding, nuclear division, and Syp1-eGFP localization. (C) Wild-type cells expressing Syp1-eGFP and Shs1-mCherry were filmed at room temperature with 1-min time lapse. Z-stacks (31 planes at 0.2- $\mu$ m spacing) were maximum projected and deconvolved with Huygens. Arrowheads indicate the appearance of septin and Syp1 rings. (D) Images of wild-type cells expressing Syp1-eGFP and Shs1-mCherry show that Syp1 rings are larger in diameter than Shs1 rings and located on mother side of the bud neck. (E) Schematic representation of the Syp1 protein showing the N-terminal F-BAR domain (yellow), the middle, unstructured region (white) containing the proline-rich domain (gray), and the muniscin-homology domain (green) at the C-terminus. Pink boxes indicate the two phospholipid-binding motifs, and asterisks mark the position of the serines phosphorylated by Pkc1. (F) The three domains of Syp1 were purified from bacteria (purified proteins are shown on top after Coomassie blue staining of an acrylamide gel) and subjected to *in vitro* phosphorylation by wild-type or kinase-dead (kd) Pkc1 immunoprecipitated from yeast cells ( $[\gamma\text{-}^{33}\text{P}]\text{ATP}$  labeling, bottom). (G) Syp1-HA3 was immunoprecipitated from protein extracts obtained from cycling cultures of strains with the indicated genotypes and probed by Western blot with a phospho-specific antibody raised against phosphorylated Ser-347, as well as with anti-HA antibodies.

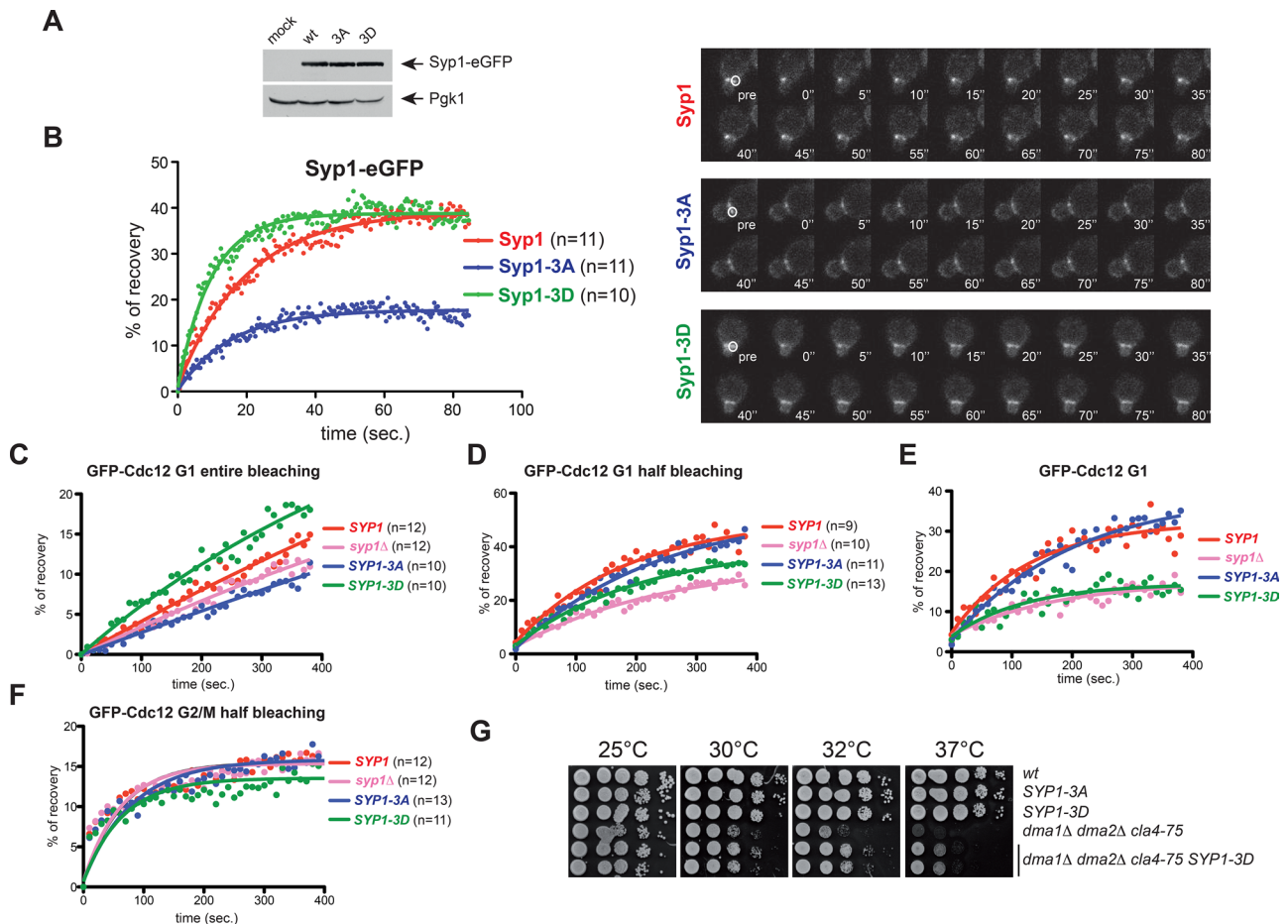


**FIGURE 6:** Syp1 phosphorylation by Pkc1 promotes Syp1 turnover at the bud neck and rigidity of the septin ring during its formation. (A) Steady-state levels of Syp1-, Syp1-3A-, and Syp1-3D-eGFP in logarithmically growing cells. (B) FRAP analysis of Syp1-eGFP at the bud neck. Half of the Syp1 ring was bleached in small-budded wild-type, *SYP1-3A*, and *SYP1-3D* cells, and recovery of fluorescence was measured every 0.5 s. Time 0 indicates the first time point after bleaching. Curves were fitted to monoexponential decay. (C–F) Cells with the indicated genotypes and expressing GFP-Cdc12 were analyzed by FRAP after bleaching of the entire (C) or half septin ring (D, F) in either G1 cells (C, D) or G2/M cells (F). Images were taken every 10 s. Time 0 corresponds to the first frame after bleaching. Curves were fitted with a one-phase association function (C, D) or with a two-phase association function (F). The goodness of the fit was based on 95% confidence intervals and  $R^2$  values. Kinetics of recovery after entire bleaching (C) was subtracted from those after half-bleaching (D) to obtain curves of recovery deriving only from septin dynamics inside the ring (i.e., recovery from the unbleached half of the ring; E). (G) Serial dilutions of stationary-phase cultures of strains with the indicated genotypes were spotted on YEPD plates and incubated for 2 d at the indicated temperatures.

promotes septin ring fluidity during its assembly. Consistent with these ideas, the *SYP1-3D* allele partially suppressed the temperature sensitivity of the *dma1Δ dma2Δ cla4-75* triple-mutant cells (Figure 6G). No significant differences were found between wild-type and *SYP1* mutants in the curves of recovery after half-bleaching in budded cells (i.e., in S/G2/M; Figure 6F). Thus phosphorylation of Syp1 may affect septin dynamics most specifically before or at the time of bud emergence, that is, when the plasma membrane remodels at the bud neck and concomitant with septin structures being under mechanical stress.

Having found that septin ring fluidity is affected by Syp1 phosphorylation prompted us to test whether *SYP1* phosphomutants undergo normal septin ring assembly in late G1. To this end, we quantitatively measured deposition of GFP-Cdc12 at the presumptive bud site by time-lapse video microscopy of cells released from G1 into the cell cycle at 30°C. The *syp1Δ*, *SYP1-3A*, and *SYP1-3D* single-mutant cells all recruited GFP-Cdc12 at the future bud site

more slowly than do wild-type cells (Figure 7A), suggesting that proper turnover of Syp1 at the bud neck upon phosphorylation by Pkc1 is required for timely building of a robust septin ring.

### Syp1 interacts with and might regulate the activity of the cell wall-remodeling enzyme 1,3-β-D-glucan synthase

To gain insights into the mechanism by which Syp1 modulates septin dynamics, we searched for Syp1-interacting proteins by mass spectrometry. To this end, we tagged Syp1 with a triple-Flag tag (Syp1-3Flag) and immunoprecipitated from wild-type and *pkc1Δ* cells growing in 1% yeast extract, 2% bactopectone, 50 mg/l adenine medium supplemented with 2% glucose (YEPD) containing sorbitol. Immunoprecipitated material was then separated by SDS-PAGE and analyzed by tandem mass spectrometry (MS/MS). Although Syp1 was found to interact with septins by protein-fragment complementation assays (Tarassov *et al.*, 2008) and *in vitro* pull downs (Qiu *et al.*, 2008), we could never find any septins in our

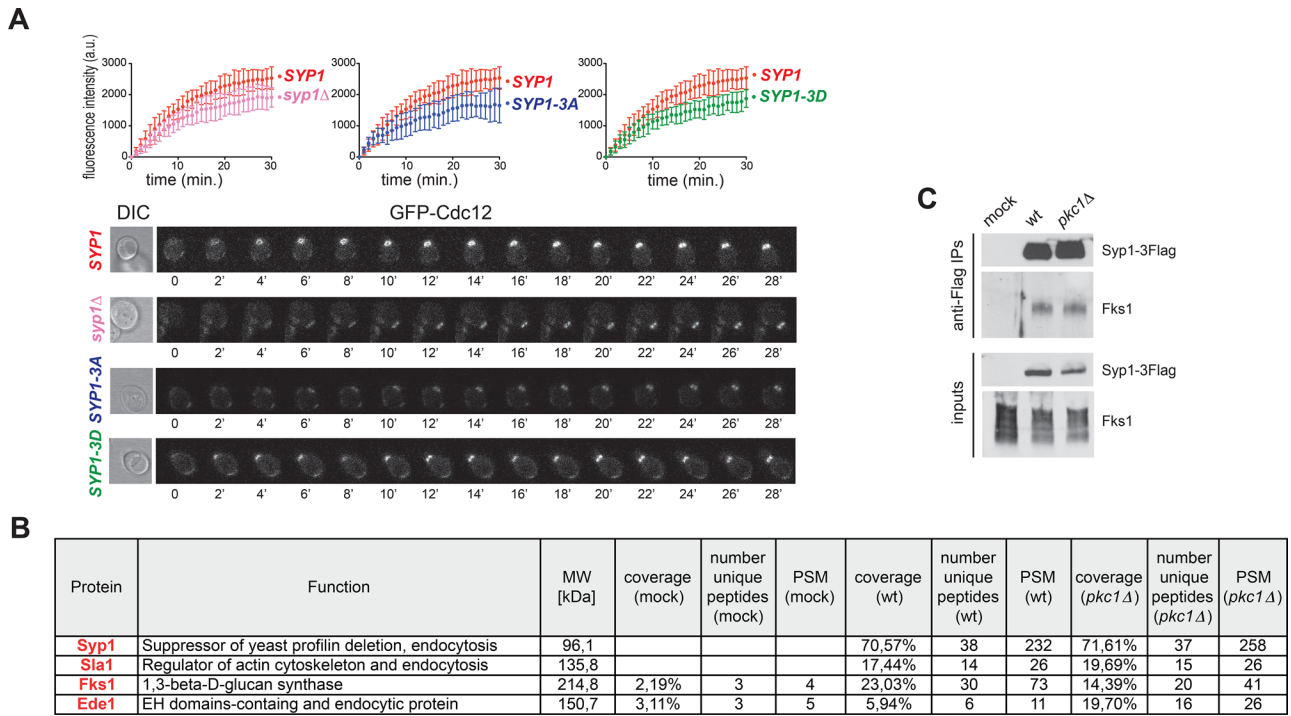


**FIGURE 7:** *Syp1* contributes to fast septin recruitment at the bud neck and interacts with *Fks1*. (A) Kinetics of septin recruitment at the presumptive bud site were calculated by measuring the fluorescence intensity of GFP-Cdc12 over time (frames every 1 min) in cells with the indicated genotypes arrested in G1 by  $\alpha$ -factor and released into fresh medium at 30°C at time 0. Wild type,  $n = 9$ ; *syp1Δ*,  $n = 18$ ; *SYP1-3A*,  $n = 10$ ; *SYP1-3D*,  $n = 15$ . (B) Mass spectrometric analysis of Flag immunoprecipitates from cell extracts of wild-type cells expressing either untagged *Syp1* (mock) or Flag-tagged *Syp1* (*Syp1-3xFlag*) and carrying either wild-type *PKC1* or *PKC1* deletion (*pkc1Δ*). Cells were grown to exponential phase in sorbitol-containing medium to keep *pkc1Δ* cells alive. The table contains only a partial list of *Syp1*-interacting proteins that were uncovered by mass spectrometry. Unique peptides are peptides with different amino acid sequence. PSM (peptide-spectrum match) represents the total number of peptides identified for each protein. (C) *Syp1-3Flag* was immunoprecipitated from wild-type and *pkc1Δ* cells grown in YEPD containing sorbitol. Immunoprecipitates were separated by SDS-PAGE electrophoresis and analyzed by Western blot with anti-*Fks1* and anti-Flag antibodies.

*Syp1-3Flag* purifications (unpublished data). Instead, we found several endocytic factors associated to *Syp1*, among which were *Sla1* and *Ede1*, which are known *Syp1* interactors (Gavin *et al.*, 2002; Reider *et al.*, 2009; Figure 7B and Supplemental Table S2). Surprisingly, among the best hits, we also found *Fks1*, the major yeast 1,3- $\beta$ -D-glucan synthase, which is involved in cell wall synthesis and is an effector of *Rho1* (Douglas *et al.*, 1994; Qadota *et al.*, 1996). Furthermore, *Fks1* has been implicated in endocytosis, along with *Rho1* (deHart *et al.*, 2003). We confirmed the association between *Syp1* and *Fks1* by immunoprecipitation of *Syp1-3Flag* followed by Western blot analysis with anti-*Fks1* antibodies (Figure 7C). Furthermore, similar levels of *Fks1* were coimmunoprecipitated with *Syp1-3Flag* from wild-type and *pkc1Δ* cells (Figure 7C), indicating that *Pkc1* does not affect *Fks1* association with *Syp1*.

Because 1,3- $\beta$ -D-glucan synthase contributes to proper septin distribution in the pathogenic budding yeast *Candida albicans* (Blankenship *et al.*, 2010; Badrane *et al.*, 2012), the association between *Syp1* and *Fks1* suggests that these proteins might cooperate in controlling septin ring formation.

## DISCUSSION

### Rho1 functions in the control of septin organization

In metazoans and yeasts, the small Rho-family GTPase *RhoA/Rho1* is a central regulator of cytokinesis. In all of these organisms, it

promotes the assembly and contraction of the actomyosin ring, partly through activation of formins (reviewed in Piekny *et al.*, 2005). Here we show that budding yeast *Rho1* has an unanticipated role in cytokinesis by controlling septin dynamics. Indeed, we show, by a number of different approaches, that a novel dominant allele of *RHO1*, *RHO1-D72N*, stabilizes the septin ring at the bud neck. The *RHO1-D72N* mutation replaces an Asp residue located inside the switch II and conserved in all of the GTPases of the Rho family. The switch I and the switch II are GTPase domains that undergo the most dramatic structural rearrangements upon GTP binding and hydrolysis and cooperate to promote GTPase activation. In addition, these regions modulate the interactions of GTPases with their GAPs and effectors (Vetter and Wittinghofer, 2001). Thus the D72N amino acid substitution could modify *Rho1* structure, leading to a *Rho1* hyperactive variant that could stabilize the interaction with GTP, promote the interaction with a specific guanine nucleotide exchange factor (GEF), inhibit the binding to a GAP, and/or increase the affinity to specific effector(s). Although another Rho GTPase, *Cdc42*, is required for septin recruitment to the presumptive bud site (Gladfelter *et al.*, 2002; Caviston *et al.*, 2003; Iwase *et al.*, 2006; Okada *et al.*, 2013), a synonymous amino acid change in *Cdc42* (*Cdc42-D65N*; Mosch *et al.*, 2001) does not have the same effect on septin stability, suggesting that *Rho1* and *Cdc42* play distinct functions in septin organization. The finding that mutations locking

Cdc42 in the active, GTP-bound state cause septin misorganization (Gladfelter *et al.*, 2002; Caviston *et al.*, 2003) further supports this conclusion.

### **Pkc1 as a central effector of Rho1 in the regulation of septin ring stability**

We provide several lines of evidence indicating that Pkc1 is a key effector of Rho1 in the regulation of septin recruitment and ring formation at the bud neck. First, Pkc1 hyperactivation through the well-characterized *PKC1-R398P* allele (Nonaka *et al.*, 1995) phenocopied the effects of *RHO1-D72N* on septin stability. Second, five different dominant mutations in our initial suppressor screen mapped in the *PKC1* gene. Third, *PKC1* deletion destabilizes septin collars, as shown by FRAP. Our finding that lack of Pkc1 is lethal for septin mutants even in the presence of an osmostabilizer further corroborates the notion that Pkc1 stabilizes the septin ring. Note that the real contribution of Pkc1 to septin ring stability under normal conditions might be underestimated in our experiments by the addition to the medium of sorbitol, which we show stabilizes septins at the bud neck. In our hands, conditional *pkc1* mutant cells (Anastasia *et al.*, 2012; unpublished data) rapidly lose viability and lyse in the absence of osmostabilizers similar to *pkc1Δ* cells, thus hampering a rigorous assessment of the effect of Pkc1 on septin regulation.

We cannot exclude that Rho1 contributes to septin ring assembly and stabilization also via additional effectors besides Pkc1. For instance, deletion of the formin Bni1 was shown to cause defects in septin organization and larger septin rings (Kadota *et al.*, 2004). However, Bni1 is activated mainly by Rho3 and Rho4 at physiological temperatures (Dong *et al.*, 2003), and its localization requires Cdc42 activity (Jaquenoud and Peter, 2000; Ozaki-Kuroda *et al.*, 2001). In spite of Rho1 and Bni1 displaying two-hybrid interactions, Rho1 appears to activate Bni1 only at high temperatures and through an indirect mechanism that requires Pkc1 (Dong *et al.*, 2003; Kono *et al.*, 2012). Similarly, although Rho1 activates the  $\beta$ -1,3-glucan synthase encoded by the *FKS1* and *FKS2* genes (Qadota *et al.*, 1996) for the cell wall synthesis (Douglas *et al.*, 1994; Inoue *et al.*, 1996), our data suggest that Fks1 activity might be further regulated by the Pkc1 target, Syp1. Other effectors of Rho1, such as the Sec3 subunit of the exocyst complex (Guo *et al.*, 2001), which mediates polarized targeting and tethering of secretory vesicles (TerBush *et al.*, 1996), have not been implicated in septin regulation. Thus we favor the idea that Pkc1 is a critical effector of Rho1 in the control of septin organization.

Circumstantial evidence suggests that septin regulation by protein kinase C (PKC) might be operational in other systems. Indeed, dendritic spine morphogenesis requires both septins (Tada *et al.*, 2007; Xie *et al.*, 2007) and atypical PKC (aPKC; Zhang and Macara, 2008). Besides promoting biogenesis of primary cilia in epithelial cells (Fan *et al.*, 2004) and motile cilia in sea urchin, aPKC forms a ring at the base of the latter cilium (Pruliere *et al.*, 2011) that is reminiscent of the ring-like septin structure found at the base of cilia (Hu *et al.*, 2010; Kim *et al.*, 2010). Finally, mammalian Sept2 is efficiently phosphorylated *in vitro* by PKC (Xue *et al.*, 2000). Further studies will help to shed light on the links between PKC and septins in dendrite arborization, ciliogenesis, and sperm morphogenesis.

### **The F-BAR protein Syp1 and the control of septin dynamics**

We identified the membrane protein Syp1 as a novel bona fide target of Pkc1. Syp1 is a member of the Bin-amphiphysin-Rvs (BAR) family of membrane proteins, which sculpt phosphoinositide-rich membranes to promote membrane curvature. Because of their abil-

ity to sense and modulate such curvature, BAR proteins are implicated in numerous processes involving membrane reorganization, such as endocytosis, cell migration, and cytokinesis (Suetsugu *et al.*, 2010).

Syp1 exhibits a peculiar localization, forming a ring in late G1 that surrounds the new-forming septin ring and might define a specific membrane domain. Thus, after budding, the Syp1 ring ends up being larger than the septin ring. Of interest, establishment of cell polarity in yeast has been recently linked to the spatial coordination of exocytosis and endocytosis at the presumptive bud site. Specifically, an exocytic cortical pole is encircled by an endocytic ring rich in actin patches that confines exocytosis to a polarity vertex (Jose *et al.*, 2013). How the septin ring is spatially organized in relation to these membrane compartments has not been addressed directly, but the septin ring likely coincides with the endocytic ring, on the basis of their respective diameters and the evidence that exocytosis is required to poke a hole in the septin cap during ring formation (Okada *et al.*, 2013). Being external to the septin ring, the Syp1 ring could in turn influence the rate of local endocytosis and/or septin recruitment by preventing the lateral spreading of these processes.

Syp1 was shown to interact physically with septins and accelerate septin turnover (Qiu *et al.*, 2008). Consistently, we show that lack of Syp1 suppressed the temperature sensitivity of mutants defective in septin ring assembly. Another yeast F-BAR protein, Hof1, controls actomyosin ring dynamics and cytokinesis (Lippincott and Li, 1998; Meitinger *et al.*, 2011). Similar to Syp1, Hof1 localizes to the bud neck early during the cell cycle and affects the integrity of septin assemblies (Lippincott and Li, 1998; Meitinger *et al.*, 2011), suggesting that besides stabilizing the actomyosin ring, it might share a function with Syp1 in septin regulation. Strikingly, we find that simultaneous inactivation of *HOF1* and *SYP1* is lethal (unpublished data), further strengthening this hypothesis.

BAR proteins, including Syp1, cluster PI(4,5)P<sub>2</sub> (Saarikangas *et al.*, 2009) and prevent its lateral diffusion, thus stabilizing lipid microdomains (Zhao *et al.*, 2013). Because PI(4,5)P<sub>2</sub> is concentrated at the bud neck (Garrenton *et al.*, 2010) and stimulates septin filament assembly and organization (Bertin *et al.*, 2010), it is tempting to speculate that BAR proteins might play a general role in the control of septin assemblies. The F-BAR protein syndapin/pacsin, which is a known PKC target (Plomann *et al.*, 1998), promotes dendritic spine morphogenesis in neurons (Dharmalingam *et al.*, 2009) and cytokinesis in *Drosophila* (Takeda *et al.*, 2013). An exciting possibility is that these functions might be linked to a possible role of syndapin/pacsin in coordination of septin dynamics with membrane reorganization.

Here we show that Syp1 is phosphorylated by Pkc1 *in vitro* and, presumably, *in vivo* on Ser-347, -389, and/or -390 within a basic domain of the protein that contains two consensus motifs for phospholipid binding outside of the F-BAR domain. This region of the protein was previously shown to contribute to Syp1 localization at the plasma membrane (Reider *et al.*, 2009). Pkc1-dependent phosphorylation of these serines accelerates the turnover of Syp1 at the bud neck. In agreement with the proposed role of Syp1 in promoting septin dynamics (Qiu *et al.*, 2008), our data indicate that increasing Syp1 turnover at the bud neck with the *SYP1-3D* allele renders septins less mobile within the new-forming septin ring in late G1, that is, during a cell cycle stage in which the septin ring is usually in a fluid state and characterized by free lateral diffusion (Caviston *et al.*, 2003; Dobbelaere *et al.*, 2003).

Unlike *PKC1* deletion, the *SYP1-3A* mutant allele does not obviously affect septin ring stability and does not cause synthetic lethality or sickness to septin mutants (unpublished data), indicating

that it impairs septin organization to a lower extent than Pkc1 inactivation. One possible explanation is that additional Syp1 residues besides Ser-347, -389, and -390 might be phosphorylated by Pkc1. Furthermore, Pkc1 might have additional targets besides Syp1 in septin regulation. One intriguing possibility to be investigated in the future is whether Hof1 is also a Pkc1 phosphorylation target.

### Possible mechanisms of septin regulation by Syp1 and other BAR proteins

Given their nature as membrane sculptors, an attractive model is that BAR proteins remodel both membrane and septins while membrane curvature changes.

Although the exact mechanism by which Syp1 controls septin dynamics remains to be established, we can envision several possibilities. First, Syp1 might influence the formation of septin filaments or their organization into a ring through direct interaction with septins (Qiu *et al.*, 2008). Second, Syp1 might contribute to organizing septin assemblies at the presumptive bud site by regulating the local concentration of PI(4,5)P<sub>2</sub>. A third, non-mutually exclusive hypothesis is that Syp1 controls septin recruitment and efficient septin ring assembly through endocytic recycling of septins, which is consistent with the established involvement of Syp1 in endocytosis (Boettner *et al.*, 2009; Reider *et al.*, 2009; Stimpson *et al.*, 2009). For instance, Syp1 could help to focus septin recruitment to the site of highest membrane curvature, that is, the bud neck. Although at a first glance this hypothesis might seem at odds with the different diameters expected for the Syp1 and the endocytic ring involved in polarity establishment (Jose *et al.*, 2013), Syp1 could mediate a qualitatively different endocytosis relative to the one involved in polarity and, unlike the latter, prevent septins from spreading out. In this context, it is interesting to note that Rho1 was implicated in a novel clathrin-independent endocytic pathway that involves actin cables but not patches (Prosser *et al.*, 2011). Moreover, the 1,3- $\beta$ -D-glucan synthase Fks1, which we show interacts with Syp1, has been implicated in endocytosis independently of its cell wall-remodeling function (Okada *et al.*, 2010). Further work will be required to establish whether the role of Syp1 in septin regulation is linked to its endocytic function.

Syp1 interaction with Fks1, which synthesizes the main cell wall component and is in turn regulated by Rho1 activity, suggests yet another possible mechanism underlying septin regulation. As mentioned earlier, Rho1, Pkc1, and Fks1 are part of the CWI pathway, which responds to a variety of environmental changes, including mechanical stress caused by cell wall defects (Levin, 2011). Signals are initiated at the cell surface by mechanosensors, such as Mid2 and Wsc1, which localize across the membrane and surrounding periplasmic space. Signals are then transduced to the Rho1 GEFs Rom1 and Rom2 at the plasma membrane, triggering activation of Rho1 and its effectors. Our data suggest that the upstream part of the CWI pathway is involved in septin ring stabilization at least partly through Syp1 phosphorylation. Of importance, the CWI pathway is induced not only under stress conditions, but also during the normal cell cycle, concomitant with polarized growth and bud emergence (Zarrov *et al.*, 1996), that is, when cells undergo the most pronounced membrane/cell wall remodeling and are most vulnerable to lysis. Of note, this is also the cell cycle phase when the septin ring undergoes the transition from fluid to frozen state. Thus it would make perfect sense that the same Rho1/Pkc1 pathway couples new cell wall synthesis with septin ring stability. Intriguingly, Syp1 interacts with the mechanosensor Mid2 (Reider *et al.*, 2009), suggesting that it might itself relay mechanical stress signals, acting as a mechanotransducer and/or participating in a Rho1-controlling feedback

loop. Glucan synthesis could then stiffen the cell wall and, consequently, stabilize the septin ring. Consistent with this hypothesis, in the pathogenic fungus *C. albicans*, cell treatment with the glucan synthase inhibitor caspofungin leads to septin mislocalization (Blankenship *et al.*, 2010; Badrane *et al.*, 2012). Our finding that septin defects can be suppressed by addition of the osmostabilizer sorbitol to the medium further supports the idea of intimate cross-talk between cell wall and septin organization. In this scenario, cell wall reorganization by Rho1/Pkc1 would be part of a physiological circuit responding to mechanical stress and stabilizing the cytokinetic machinery either during the normal cell cycle or upon cell wall injury. This mechanism might be conserved, as suggested by recent data showing that mechanical stress stabilizes cytokinetic factors at the cleavage furrow in *Dictyostelium* cells (Srivastava and Robinson, 2015).

In conclusion, we have identified a novel pathway controlling septin dynamics in yeast. Given the evolutionary conservation of some of the players, similar pathways might be involved in controlling septin dynamics in other systems, such as dendritic spines and cilia.

## MATERIALS AND METHODS

### Strains, media, reagents, and genetic manipulations

All yeast strains were derivatives of W303 (*ade2-1, trp1-1, leu2-3112, his3-11,15, ura3, ssd1*). W303 bears a frameshift mutation in the *BUD4* gene (Voth *et al.*, 2005), which encodes an anillin-related protein that stabilizes the septin ring during splitting (Wloka *et al.*, 2011). For some critical mutants, we made *BUD4*<sup>+</sup> versions in W303. A full list of strains and plasmids used in this study is given in Supplemental Table S3. Unless specified, most strains were generated in the original *bud4* W303 background. Cells were grown in either synthetic minimal medium supplemented with the appropriate nutrients, YEPD, or YEPD + 1 M sorbitol.  $\alpha$ -Factor was used at 2  $\mu$ g/ml and nocodazole at 15  $\mu$ g/ml. Standard techniques were used for genetic manipulations (Sherman, 1991; Maniatis *et al.*, 1992). Gene deletions were generated by one-step gene replacement (Wach *et al.*, 1994). One-step tagging techniques (Janke *et al.*, 2004; Sheff and Thorn, 2004) were used to create triple hemagglutinin (3xHA)-, 3xFlag-, and eGFP-tagged Syp1. *SYP1* phosphorylation mutants were obtained by site-directed mutagenesis using the QuikChange Mutagenesis Kit (Agilent Technologies, Santa Clara, CA). Integration of *SYP1* alleles into the genome was checked by Southern blot.

### Mutagenesis with ethyl methanesulfonate and isolation of *RHO1-D72N* allele

The temperature sensitivity of *dma1 $\Delta$  dma2 $\Delta$  cla4-75* cells in the W303 background was unaffected by replacing the defective endogenous *bud4* allele with wild-type *BUD4* (Supplemental Figure S1A). For mutagenesis, a cellular suspension of *dma1 $\Delta$  dma2 $\Delta$  cla4-75 bud4* cells was treated with 3% ethyl methanesulfonate for 60 min. Cells were plated on YEPD plates at 37°C to isolate thermoresistant suppressors. Temperature-resistant clones were assessed for the ability to lose the *cla4-75* allele carried on an episomal centromeric plasmid by replica plating on 5-fluoroorotic acid (5-FOA) plates to select their derivatives lacking the *cla4-75* construct. After this secondary screen, 44 suppressors that retained viability in face of the simultaneous lack of Dma1, Dma2, and Cla4 were recovered.

Dominance/recessivity of the suppressing mutations was assessed by crossing suppressors with the parental strain (*dma1 $\Delta$  dma2 $\Delta$  cla4-75*). Derivative diploids were selected and analyzed for their ability to grow at 37°C and on 5-FOA.

To identify *RHO1-D72N* as a suppressing allele, we constructed a genomic library from one of the dominant suppressors by partial digestion of its genomic DNA with *Sau3A* followed by ligation of 8.0- to 12.0-kb DNA fragments into *Bam*HI of *Ycplac111*. This genomic library was then used to transform the *dma1Δ dma2Δ cla4-75* parental strain, and plasmids carrying the *RHO1-D72N* allele were isolated by virtue of their ability to confer temperature and 5-FOA resistance to *dma1Δ dma2Δ cla4-75* cells. Suppression was confirmed after subcloning the *RHO1-D72N* allele in *Ycplac111*.

### FRAP and fluorescence microscopy

FRAP experiments in Figure 3, A–C, and Supplemental Figure 6, C–F, were performed as previously described (Dobbelaere *et al.*, 2003) on a Zeiss LSM510 (Zeiss, Jena, Germany) confocal microscope. Logarithmically growing cells expressing GFP-Cdc12 were grown overnight in YEPD, resuspended in synthetic complete medium, and spread on 2% agar pads. Half or the entire septin ring was bleached with a sequence of 20–25 iterations at 50% of laser intensity. Fluorescence recovery was recorded over time at 30 or 37°C (experiments in Figure 3B), and fluorescence intensities were analyzed with ImageJ (National Institutes of Health, Bethesda, MD). Background staining in each cell was subtracted. To correct for general bleaching, fluorescence intensities of septin rings were normalized to those of two or three reference cells present in each movie.

FRAP experiments in Figure 6B were performed on a Zeiss LSM780 confocal microscope equipped with a Definite Focus module and controlled by the Zen2010 software (Zeiss). Logarithmically growing cells expressing Syp1-eGFP were grown overnight in synthetic complete medium at 30°C and mounted on Fluorodishes (World Precision Instruments, Sarasota, FL). Half of the Syp1 ring was bleached in small-budded cells with a sequence of five iterations at 100% of laser intensity. Fluorescence recovery was recorded every 0.5 s at 30°C, and fluorescence intensities were analyzed with ImageJ. Background staining in each cell was subtracted. Data were fitted to monoexponential decay with Prism5 (GraphPad Software, San Diego, CA) to calculate the mobile fraction and the half recovery time.

For time-lapse video microscopy in Figure 3F, cells were imaged at 30°C on 2% agar pads of complete synthetic medium. Movies were recorded with a DeltaVision microscope and a 100× oil immersion objective using SoftWoRx software (GE Healthcare, Velizy-Villacoublay, France). Individual Z-stacks contained 10 planes with a step size of 0.6 μm and were binned symmetrically by two. After image acquisition, the movies were projected as maximum intensity projections.

For time-lapse video microscopy in Supplemental Figures S3 and S5C, cells were mounted in synthetic medium on Fluorodishes and filmed at room temperature (~22°C) with a DeltaVision OMX (GE Healthcare) using a 63× oil immersion objective using SoftWoRx software. Individual Z-stacks containing 31 planes were acquired every 1 min with a step size of 0.2 μm and were binned symmetrically by one. Z-stacks were maximum projected and deconvolved with Huygens (Scientific Volume Imaging, Hilversum, Netherlands).

For time-lapse video microscopy in Figure 3H, cells were mounted in synthetic medium on Fluorodishes and filmed at 30°C with a 100× oil immersion objective mounted on a confocal spinning disk CSU-X1 Andor-Nikon microscope (Nikon, Tokyo, Japan) equipped with an electron-multiplying charge-coupled device (CCD) iXon Ultra camera and controlled by Andor iQ3 software. Individual Z-stacks contained eight planes with a step size of 0.7 μm and were acquired every 1 min. Fluorescence intensities of GFP-Cdc12 were measured with ImageJ on maximum projected images.

For time-lapse video microscopy in Figure 7A, cells were mounted in synthetic medium on Fluorodishes and filmed at 30°C with 63× oil immersion objective mounted on a Zeiss LSM780 confocal microscope controlled by the Zen2010 software. Individual Z-stacks contained eight planes with a step size of 0.7 μm and were acquired every 1 min. Fluorescence intensities of GFP-Cdc12 were measured with ImageJ on maximum projected images.

Nuclear division was scored on cells stained with propidium iodide.

Visualization of septin or Syp1-HA3 rings was performed on formaldehyde-fixed cells using anti-Cdc11 polyclonal antibodies (Santa Cruz Biotechnology, Dallas, TX) or anti-HA monoclonal antibody (12CA5) as previously described (Merlini *et al.*, 2012). Still digital images were taken with an oil 63×, 1.4-0.6 HCX Plan-Apochromat objective (Zeiss) with a CoolSNAP HQ2-1 CCD camera (Photometrics, Tucson, AZ) mounted on a Zeiss AxioimagerZ1/Apoptome fluorescence microscope controlled by the MetaMorph imaging system software (Molecular Devices, Silicon Valley, CA).

### Protein purification, immunoprecipitations, and kinase assays

Purification of histidine-tagged Syp1 truncated proteins was performed as previously described (Reider *et al.*, 2009). For use in kinase assays, proteins were dialyzed in 20 mM 4-(2-hydroxyethyl)-1-piperazineethanesulfonic acid, pH 7.4, and 50 mM NaCl and concentrated using centrifugal filter units (10-kDa MWCO; Millipore, Darmstadt, Germany).

For immunoprecipitations of HA-tagged Syp1, pellets from 50-ml yeast cultures (10<sup>7</sup> cells/ml) were lysed at 4°C with acid-washed glass beads in lysis buffer (50 mM Tris-Cl, pH 7.5, NaCl 150 mM, 10% glycerol, 1 mM EDTA, and 1% NP-40, supplemented with protein inhibitors [Complete; Roche, Basel, Switzerland], 1 mM Na orthovanadate, and 60 mM β-glycerophosphate). Total extracts were cleared by spinning at 12,000 rpm for 10 min and quantified by NanoDrop (Thermo Scientific, Waltham, MA). The same amounts of protein extracts were subjected to immunoprecipitation with an anti-HA affinity resin (Roche). Immunocomplexes were washed three times in lysis buffer and twice in phosphate-buffered saline (PBS) before SDS-PAGE electrophoresis.

Immunoprecipitations of Flag-tagged Syp1 were performed in TBSN buffer (25 mM Tris-Cl, pH 7.4, 100 mM NaCl, 2 mM EDTA, 0.1% NP-40, 1 mM dithiothreitol [DTT]) supplemented with protein inhibitors (Complete) and phosphatase inhibitors (PhosStop; Roche) using protein G Dynabeads (Life Technologies, Carlsbad, CA) cross-linked to the M2 monoclonal anti-Flag antibody (Sigma-Aldrich, St. Louis, MO). Immunocomplexes were washed four times in TBSN and twice in PBS before elution with 0.5 mg/ml 3xFlag peptide in 50 mM Tris-Cl, pH 8.3, 1 mM EDTA, and 0.1% SDS.

Pkc1 immunoprecipitations and kinase assays were performed essentially as described (Watanabe *et al.*, 1994), except that a high-salt buffer was used for cell lysis. Briefly, wild-type or kinase-dead (K853R) HA-tagged Pkc1 (Watanabe *et al.*, 1994) was overexpressed in yeast cells from the inducible *GAL1* promoter after galactose induction for 3 h at 30°C. Cells were lysed at 4°C with acid-washed glass beads in lysis buffer (50 mM Tris-Cl, pH 7.5, 1 M NaCl, 1 mM ethylene glycol tetraacetic acid, 1 mM EDTA, and 1% NP-40 supplemented with protease and phosphatase inhibitors [Complete and PhosStop]), and Pkc1 was immunoprecipitated with 12CA5 anti-HA antibodies preadsorbed on protein A-Sepharose. Immunocomplexes were washed twice with lysis buffer and once with 40 mM 3-(*N*-morpholino)propanesulfonic acid, pH 7.5. Kinase assays were

performed as described (Watanabe *et al.*, 1994) using 2  $\mu\text{g}$  of Syp1 or myelin basic protein (MBP) per reaction.

For Western blot analysis, trichloroacetic acid protein extracts were prepared as previously described (Rancati *et al.*, 2005). Proteins transferred to Protran membranes (Schleicher and Schuell, Dassel, Germany) were probed with monoclonal anti-HA 12CA5, anti-GFP (ChromoTek, Planegg-Martinsried, Germany), and anti-Pgk1 (Life Technologies) antibodies or with polyclonal anti-Fks1 antibodies (Santa Cruz Biotechnology). Phosphorylated Slt2 was detected using a monoclonal antibody against phospho-p44/42 MAPK (Cell Signaling, Danvers, MA), and total levels of Slt2 were monitored with anti-Slt2 polyclonal antibodies (Santa Cruz Biotechnology).

Secondary antibodies were purchased from GE Healthcare, and proteins were detected by an enhanced chemiluminescence system according to the manufacturer.

### Mass spectrometry analysis

The identification of Syp1 phosphorylation sites was carried out on three independent replicates. In vitro-phosphorylated Syp1 proteins were digested overnight using 1 mg of trypsin in 2 M urea and 50 mM triethylammonium bicarbonate. Resulting peptides were diluted with four volumes of 0.2% trifluoroacetic acid, loaded on C18 Agilent Bond Elut, desalted with two washes of 0.1% formic acid, eluted with 50% acetonitrile/0.1% formic acid, and dried to completeness in a SpeedVac vacuum concentrator (Thermo Scientific).

For interactome analysis, immunoprecipitates were separated on SDS-PAGE gels (12% polyacrylamide, Mini-PROTEAN TGX Precast Gels; Bio-Rad, Hercules, CA) and stained with Page Blue Stain (Euro-medex, Souffelweyersheim, France). Gel lanes were cut into six gel pieces and destained with three washes in 50% acetonitrile and 50 mM triethylammonium bicarbonate (TEABC). After protein reduction (with 10 mM DTT in 50 mM TEABC at 60°C for 30 min) and alkylation (55 mM iodoacetamide/TEABC at room temperature for 30 min), proteins were digested in-gel using trypsin (1.2  $\mu\text{g}/\text{band}$ , Gold; Promega, Madison, WI) as previously described (Shevchenko *et al.*, 1996).

Peptides were analyzed by nano-flow HPLC-nano electrospray ionization using an LTQ Orbitrap XL mass spectrometer coupled to an Ultimate 3000 HPLC (Thermo Scientific). Preconcentration of samples was performed on-line on a Pepmap precolumn (0.3 mm  $\times$  10 mm; Thermo Scientific). A gradient consisting of 2–40% buffer B (100% acetonitrile, 0.1% trifluoroacetic acid; 30 min for phosphorylation analysis, 60 min for interacting protein analysis), 40–80% B (1 min), and 80–0% B (1 min) and equilibrated for 20 min in 0% B was used to elute peptides at 300 nl/min from an Acclaim Pepmap100 C18 capillary (0.075 mm  $\times$  150 mm) reverse-phase column (Thermo Scientific). Mass spectra were acquired using a top-5 collision-induced dissociation, data-dependent-acquisition method. The LTQ-Orbitrap was programmed to perform a Fourier transform (FT) full scan (60,000 resolution) on mass range 400–1400 Th, with the top five ions from each scan selected for LTQ-MS/MS and, in the case of phosphorylation analysis, multistage activation on the neutral loss of 24.49, 32.66, and 48.99 Th. FT spectra were internally calibrated using a single lock mass (445.120024 Th). Target ion numbers were 500,000 for FT full scan on the Orbitrap and 10,000 MSn on the LTQ.

For phosphorylation analysis, Raw files were converted to Mascot generic format (MGF) using raw2MSM, version 1.07, enabling to filter the top eight ions per 100-Da mass windows. MGF files were searched with the Mascot engine, version 2.4, against the SwissProt database, version 2012\_07 (536,789 sequences), upon filtering for *S. cerevisiae* entries (7794 sequences). Modification op-

tions were fixed carbamidomethyl on cysteines and variable phosphorylation on serines/threonines and tyrosines. Mass tolerances were 7 ppm for precursor ions and 0.5 Da for fragment ions. MS2 spectra corresponding to phosphopeptides were manually inspected for phosphosite assignment. Ion signals corresponding to phosphorylated peptides were quantified from their ion chromatograms manually extracted using Qual browser, version 2.1 (Thermo Fisher Scientific), with a tolerance of 5 ppm for mass deviation and normalized to signals of their nonphosphorylated counterparts.

For interactome analysis, all MS/MS spectra were searched against the *S. cerevisiae* database (64,506 sequences, version 2013\_03, uniprot.org/) by using Proteome Discoverer software, version 1.4 (Thermo Scientific) with Mascot, version 2.4, and phosphoRS, version 3.0 nodes (Taus *et al.*, 2011). Modification options were fixed carbamidomethyl on cysteines, variable oxidation on methionines, and variable phosphorylation on serines/threonines and tyrosines. Management and validation of mass spectrometry data were performed using Proteome Discoverer software (Thermo Scientific; Mascot significance threshold  $p < 0.01$ , with a minimum of one peptide per protein). Site-specific localization of phosphorylation events was determined using the phosphoRS function of Proteome Discoverer. All spectra with pRS score  $\geq 50$  and pRS Site Probability  $\geq 0.75$  were considered. Furthermore, each phosphopeptide spectrum was manually assessed for quality.

### Other techniques

Flow cytometric DNA quantification was performed according to Fraschini *et al.* (1999) on a Becton-Dickinson FACSCalibur.

Significance of the differences was statistically tested by means of a two-tailed *t* test, assuming unequal variances. \* $p < 0.05$ , \*\* $p < 0.01$ , \*\*\* $p < 0.001$ , \*\*\*\* $p < 0.0001$ .

### ACKNOWLEDGMENTS

We are grateful to E. Bi, G. Braus, G. De Bettignies, M. Hall, T. Hoefken, B. Lapeyre, K. Lee, D. Levin, Y. Ohya, D. Pellman, M. Stark, D. Stillman, R. Tisi, and B. Wendland for sharing reagents; R. Fraschini and M. Venturetti for help with the initial phase of the genetic screen; V. Georget and J. Mateos Langerak for invaluable help with FRAP and video microscopy; the Montpellier RIO Imaging platform for image acquisition and FACS analysis; and D. Liakopoulos, S. Martin, and E. Schwob for critical reading of the manuscript. This work was supported by Grant ANR-09-BLAN-0125-01 from the Agence Nationale pour la Recherche and Grant PJA 20141201926 from the Fondation ARC to S.P. M.A.J. was supported by the Fondation pour la Recherche Médicale.

### REFERENCES

- Albuquerque CP, Smolka MB, Payne SH, Bafna V, Eng J, Zhou H (2008). A multidimensional chromatography technology for in-depth phosphoproteome analysis. *Mol Cell Proteomics* 7, 1389–1396.
- Anastasia SD, Nguyen DL, Thai V, Meloy M, Macdonough T, Kellogg DR (2012). A link between mitotic entry and membrane growth suggests a novel model for cell size control. *J Cell Biol* 197, 89–104.
- Antonsson B, Montessuit S, Friedli L, Payton MA, Paravicini G (1994). Protein kinase C in yeast. Characteristics of the *Saccharomyces cerevisiae* PKC1 gene product. *J Biol Chem* 269, 16821–16828.
- Badrane H, Nguyen MH, Blankenship JR, Cheng S, Hao B, Mitchell AP, Clancy CJ (2012). Rapid redistribution of phosphatidylinositol-(4,5)-bisphosphate and septins during the *Candida albicans* response to caspofungin. *Antimicrob Agents Chemother* 56, 4614–4624.
- Barral Y (2010). Cell biology. Septins at the nexus. *Science* 329, 1289–1290.
- Barral Y, Mermall V, Mooseker MS, Snyder M (2000). Compartmentalization of the cell cortex by septins is required for maintenance of cell polarity in yeast. *Mol Cell* 5, 841–851.

- Barral Y, Parra M, Bidlingmaier S, Snyder M (1999). Nim1-related kinases coordinate cell cycle progression with the organization of the peripheral cytoskeleton in yeast. *Genes Dev* 13, 176–187.
- Beise N, Trimble W (2011). Septins at a glance. *J Cell Sci* 124, 4141–4146.
- Berlin A, Paoletti A, Chang F (2003). Mid2p stabilizes septin rings during cytokinesis in fission yeast. *J Cell Biol* 160, 1083–1092.
- Bertin A, McMurray MA, Thai L, Garcia G 3rd, Votin V, Grob P, Allyn T, Thorner J, Nogales E (2010). Phosphatidylinositol-4,5-bisphosphate promotes budding yeast septin filament assembly and organization. *J Mol Biol* 404, 711–731.
- Blankenship JR, Fanning S, Hamaker JJ, Mitchell AP (2010). An extensive circuitry for cell wall regulation in *Candida albicans*. *PLoS Pathog* 6, e1000752.
- Bodenmiller B, Wanka S, Kraft C, Urban J, Campbell D, Pedrioli PG, Gerrits B, Picotti P, Lam H, Vitek O, et al. (2010). Phosphoproteomic analysis reveals interconnected system-wide responses to perturbations of kinases and phosphatases in yeast. *Sci Signal* 3, rs4.
- Boettner DR, D'Agostino JL, Torres OT, Daugherty-Clarke K, Uygur A, Reider A, Wendland B, Lemmon SK, Goode BL (2009). The F-BAR protein Syp1 negatively regulates WASp-Arp2/3 complex activity during endocytic patch formation. *Curr Biol* 19, 1979–1987.
- Breitkreutz A, Choi H, Sharom JR, Boucher L, Neduva V, Larsen B, Lin ZY, Breitkreutz BJ, Stark C, Liu G, et al. (2010). A global protein kinase and phosphatase interaction network in yeast. *Science* 328, 1043–1046.
- Byers B, Goetsch L (1976). A highly ordered ring of membrane-associated filaments in budding yeast. *J Cell Biol* 69, 717–721.
- Casamayor A, Snyder M (2003). Molecular dissection of a yeast septin: distinct domains are required for septin interaction, localization, and function. *Mol Cell Biol* 23, 2762–2777.
- Caudron F, Barral Y (2009). Septins and the lateral compartmentalization of eukaryotic membranes. *Dev Cell* 16, 493–506.
- Caviston JP, Longtine M, Pringle JR, Bi E (2003). The role of Cdc42p GTPase-activating proteins in assembly of the septin ring in yeast. *Mol Biol Cell* 14, 4051–4066.
- Cid VJ, Adamikova L, Sanchez M, Molina M, Nombela C (2001). Cell cycle control of septin ring dynamics in the budding yeast. *Microbiology* 147, 1437–1450.
- deHart AK, Schnell JD, Allen DA, Tsai JY, Hicke L (2003). Receptor internalization in yeast requires the Tor2-Rho1 signaling pathway. *Mol Biol Cell* 14, 4676–4684.
- DeMarini DJ, Adams AE, Fares H, De Virgilio C, Valle G, Chuang JS, Pringle JR (1997). A septin-based hierarchy of proteins required for localized deposition of chitin in the *Saccharomyces cerevisiae* cell wall. *J Cell Biol* 139, 75–93.
- Denis V, Cyert MS (2005). Molecular analysis reveals localization of *Saccharomyces cerevisiae* protein kinase C to sites of polarized growth and Pkc1p targeting to the nucleus and mitotic spindle. *Eukaryot Cell* 4, 36–45.
- Dharmalingam E, Haeckel A, Pinyol R, Schwintzer L, Koch D, Kessels MM, Qualmann B (2009). F-BAR proteins of the syndapin family shape the plasma membrane and are crucial for neuromorphogenesis. *J Neurosci* 29, 13315–13327.
- Dobbelaere J, Barral Y (2004). Spatial coordination of cytokinetic events by compartmentalization of the cell cortex. *Science* 305, 393–396.
- Dobbelaere J, Gentry MS, Hallberg RL, Barral Y (2003). Phosphorylation-dependent regulation of septin dynamics during the cell cycle. *Dev Cell* 4, 345–357.
- Dong Y, Pruyne D, Bretscher A (2003). Formin-dependent actin assembly is regulated by distinct modes of Rho signaling in yeast. *J Cell Biol* 161, 1081–1092.
- Douglas CM, Foor F, Marrinan JA, Morin N, Nielsen JB, Dahl AM, Mazur P, Baginsky W, Li W, el-Sherbeini M, et al. (1994). The *Saccharomyces cerevisiae* FKS1 (ETG1) gene encodes an integral membrane protein which is a subunit of 1,3-beta-D-glucan synthase. *Proc Natl Acad Sci USA* 91, 12907–12911.
- Fan S, Hurd TW, Liu CJ, Straight SW, Weimbs T, Hurd EA, Domino SE, Margolis B (2004). Polarity proteins control ciliogenesis via kinesin motor interactions. *Curr Biol* 14, 1451–1461.
- Fares H, Peifer M, Pringle JR (1995). Localization and possible functions of *Drosophila* septins. *Mol Biol Cell* 6, 1843–1859.
- Fraschini R, Bilotta D, Lucchini G, Piatti S (2004). Functional characterization of Dma1 and Dma2, the budding yeast homologues of *Schizosaccharomyces pombe* Dma1 and human Chfr. *Mol Biol Cell* 15, 3796–3810.
- Fraschini R, Formenti E, Lucchini G, Piatti S (1999). Budding yeast Bub2 is localized at spindle pole bodies and activates the mitotic checkpoint via a different pathway from Mad2. *J Cell Biol* 145, 979–991.
- Garrenton LS, Stefan CJ, McMurray MA, Emr SD, Thorner J (2010). Pheromone-induced anisotropy in yeast plasma membrane phosphatidylinositol-4,5-bisphosphate distribution is required for MAPK signaling. *Proc Natl Acad Sci USA* 107, 11805–11810.
- Gavin AC, Bosche M, Krause R, Grandi P, Marzioch M, Bauer A, Schultz J, Rick JM, Michon AM, Cruciat CM, et al. (2002). Functional organization of the yeast proteome by systematic analysis of protein complexes. *Nature* 415, 141–147.
- Gladfelter AS, Bose I, Zyla TR, Bardes ES, Lew DJ (2002). Septin ring assembly involves cycles of GTP loading and hydrolysis by Cdc42p. *J Cell Biol* 156, 315–326.
- Glotzer M (2005). The molecular requirements for cytokinesis. *Science* 307, 1735–1739.
- Gonzalez-Novo A, Correa-Bordes J, Labrador L, Sanchez M, Vazquez de Aldana CR, Jimenez J (2008). Sep7 is essential to modify septin ring dynamics and inhibit cell separation during *Candida albicans* hyphal growth. *Mol Biol Cell* 19, 1509–1518.
- Green RA, Paluch E, Oegema K (2012). Cytokinesis in animal cells. *Annu Rev Cell Dev Biol* 28, 29–58.
- Guo W, Tamanoi F, Novick P (2001). Spatial regulation of the exocyst complex by Rho1 GTPase. *Nat Cell Biol* 3, 353–360.
- Haarer BK, Pringle JR (1987). Immunofluorescence localization of the *Saccharomyces cerevisiae* CDC12 gene product to the vicinity of the 10-nm filaments in the mother-bud neck. *Mol Cell Biol* 7, 3678–3687.
- Hall PA, Russell SE (2012). Mammalian septins: dynamic heteromers with roles in cellular morphogenesis and compartmentalization. *J Pathol* 226, 287–299.
- Helfer H, Gladfelter AS (2006). AgSwe1p regulates mitosis in response to morphogenesis and nutrients in multinucleated *Ashbya gossypii* cells. *Mol Biol Cell* 17, 4494–4512.
- Hernandez-Rodriguez Y, Hastings S, Momany M (2012). The septin AspB in *Aspergillus nidulans* forms bars and filaments and plays roles in growth emergence and conidiation. *Eukaryot Cell* 11, 311–323.
- Holt LJ, Tuch BB, Villen J, Johnson AD, Gygi SP, Morgan DO (2009). Global analysis of Cdk1 substrate phosphorylation sites provides insights into evolution. *Science* 325, 1682–1686.
- Hu Q, Milenkovic L, Jin H, Scott MP, Nachury MV, Spiliotis ET, Nelson WJ (2010). A septin diffusion barrier at the base of the primary cilium maintains ciliary membrane protein distribution. *Science* 329, 436–439.
- Inoue SB, Qadota H, Arisawa M, Anraku Y, Watanabe T, Ohya Y (1996). Signaling toward yeast 1,3-beta-glucan synthesis. *Cell Struct Funct* 21, 395–402.
- Irie K, Takase M, Lee KS, Levin DE, Araki H, Matsumoto K, Oshima Y (1993). MKK1 and MKK2, which encode *Saccharomyces cerevisiae* mitogen-activated protein kinase-kinase homologs, function in the pathway mediated by protein kinase C. *Mol Cell Biol* 13, 3076–3083.
- Iwase M, Luo J, Nagaraj S, Longtine M, Kim HB, Haarer BK, Caruso C, Tong Z, Pringle JR, Bi E (2006). Role of a Cdc42p effector pathway in recruitment of the yeast septins to the presumptive bud site. *Mol Biol Cell* 17, 1110–1125.
- Janke C, Magiera MM, Rathfelder N, Taxis C, Reber S, Maekawa H, Moreno-Borchart A, Doenges G, Schwob E, Schiebel E, et al. (2004). A versatile toolbox for PCR-based tagging of yeast genes: new fluorescent proteins, more markers and promoter substitution cassettes. *Yeast* 21, 947–962.
- Jaquenoud M, Peter M (2000). Gic2p may link activated Cdc42p to components involved in actin polarization, including Bni1p and Bud6p (Aip3p). *Mol Cell Biol* 20, 6244–6258.
- Joberty G, Perlungher RR, Sheffield PJ, Kinoshita M, Noda M, Haystead T, Macara IG (2001). Borg proteins control septin organization and are negatively regulated by Cdc42. *Nat Cell Biol* 3, 861–866.
- Johnson ES, Blobel G (1999). Cell cycle-regulated attachment of the ubiquitin-related protein SUMO to the yeast septins. *J Cell Biol* 147, 981–994.
- Johnson ES, Gupta AA (2001). An E3-like factor that promotes SUMO conjugation to the yeast septins. *Cell* 106, 735–744.
- Jose M, Tollis S, Nair D, Sibarita JB, McCusker D (2013). Robust polarity establishment occurs via an endocytosis-based cortical coralling mechanism. *J Cell Biol* 200, 407–418.
- Kadota J, Yamamoto T, Yoshiuchi S, Bi E, Tanaka K (2004). Septin ring assembly requires concerted action of polarisome components, a PAK kinase Cla4p, and the actin cytoskeleton in *Saccharomyces cerevisiae*. *Mol Biol Cell* 15, 5329–5345.
- Kamada Y, Qadota H, Python CP, Anraku Y, Ohya Y, Levin DE (1996). Activation of yeast protein kinase C by Rho1 GTPase. *J Biol Chem* 271, 9193–9196.

- Kang PJ, Hood-DeGrenier JK, Park HO (2013). Coupling of septins to the axial landmark by Bud4 in budding yeast. *J Cell Sci* 126, 1218–1226.
- Kanshin E, Bergeron-Sandoval LP, Isik SS, Thibault P, Michnick SW (2015). A cell-signaling network temporally resolves specific versus promiscuous phosphorylation. *Cell Rep* 10, 1202–1214.
- Kim HB, Haarer BK, Pringle JR (1991). Cellular morphogenesis in the *Saccharomyces cerevisiae* cell cycle: localization of the CDC3 gene product and the timing of events at the budding site. *J Cell Biol* 112, 535–544.
- Kim SK, Shindo A, Park TJ, Oh EC, Ghosh S, Gray RS, Lewis RA, Johnson CA, Attie-Bittach T, Katsanis N, et al. (2010). Planar cell polarity acts through septins to control collective cell movement and ciliogenesis. *Science* 329, 1337–1340.
- Kinoshita M, Kumar S, Mizoguchi A, Ide C, Kinoshita A, Haraguchi T, Hiraoka Y, Noda M (1997). Nedd5, a mammalian septin, is a novel cytoskeletal component interacting with actin-based structures. *Genes Dev* 11, 1535–1547.
- Kissel H, Georgescu MM, Larisch S, Manova K, Hunnicutt GR, Steller H (2005). The Sept4 septin locus is required for sperm terminal differentiation in mice. *Dev Cell* 8, 353–364.
- Kono K, Saeki Y, Yoshida S, Tanaka K, Pellman D (2012). Proteasomal degradation resolves competition between cell polarization and cellular wound healing. *Cell* 150, 151–164.
- Kozubowski L, Panek H, Rosenthal A, Bloecher A, DeMarini DJ, Tatchell K (2003). A Bni4-Glc7 phosphatase complex that recruits chitin synthase to the site of bud emergence. *Mol Biol Cell* 14, 26–39.
- Kuo YC, Lin YH, Chen HI, Wang YY, Chiou YW, Lin HH, Pan HA, Wu CM, Su SM, Hsu CC, et al. (2012). SEPT12 mutations cause male infertility with defective sperm annulus. *Hum Mutat* 33, 710–719.
- Lam C, Santore E, Lavoie E, Needleman L, Fiacco N, Kim C, Neiman AM (2014). A visual screen of protein localization during sporulation identifies new components of prospore membrane-associated complexes in budding yeast. *Eukaryot Cell* 13, 383–391.
- Lee PR, Song S, Ro HS, Park CJ, Lippincott J, Li R, Pringle JR, De Virgilio C, Longtine MS, Lee KS (2002). Bni5p, a septin-interacting protein, is required for normal septin function and cytokinesis in *Saccharomyces cerevisiae*. *Mol Cell Biol* 22, 6906–6920.
- Levin DE (2011). Regulation of cell wall biogenesis in *Saccharomyces cerevisiae*: the cell wall integrity signaling pathway. *Genetics* 189, 1145–1175.
- Levin DE, Bowers B, Chen CY, Kamada Y, Watanabe M (1994). Dissecting the protein kinase C/MAP kinase signalling pathway of *Saccharomyces cerevisiae*. *Cell Mol Biol Res* 40, 229–239.
- Li X, Gerber SA, Rudner AD, Beausoleil SA, Haas W, Villen J, Elias JE, Gygi SP (2007). Large-scale phosphorylation analysis of alpha-factor-arrested *Saccharomyces cerevisiae*. *J Proteome Res* 6, 1190–1197.
- Lippincott J, Li R (1998). Dual function of Cyk2, a cdc15/PSTPIP family protein, in regulating actomyosin ring dynamics and septin distribution. *J Cell Biol* 143, 1947–1960.
- Longtine MS, Fares H, Pringle JR (1998). Role of the yeast Gin4p protein kinase in septin assembly and the relationship between septin assembly and septin function. *J Cell Biol* 143, 719–736.
- Maniatis T, Fritsch EF, Sambrook J (1992). *Molecular Cloning: A Laboratory Manual*, Cold Spring Harbor, NY: Cold Spring Harbor Laboratory Press.
- Marquitz AR, Harrison JC, Bose I, Zyla TR, McMillan JN, Lew DJ (2002). The Rho-GAP Bem2p plays a GAP-independent role in the morphogenesis checkpoint. *EMBO J* 21, 4012–4025.
- McMurray MA, Bertin A, Garcia G 3rd, Lam L, Nogales E, Thorner J (2011). Septin filament formation is essential in budding yeast. *Dev Cell* 20, 540–549.
- McMurray MA, Thorner J (2008). Septin stability and recycling during dynamic structural transitions in cell division and development. *Curr Biol* 18, 1203–1208.
- Meitinger F, Boehm ME, Hofmann A, Hub B, Zentgraf H, Lehmann WD, Pereira G (2011). Phosphorylation-dependent regulation of the F-BAR protein Hof1 during cytokinesis. *Genes Dev* 25, 875–888.
- Merlini L, Fraschini R, Boettcher B, Barral Y, Lucchini G, Piatti S (2012). Budding yeast dma proteins control septin dynamics and the spindle position checkpoint by promoting the recruitment of the Elm1 kinase to the bud neck. *PLoS Genet* 8, e1002670.
- Mosch HU, Kohler T, Braus GH (2001). Different domains of the essential GTPase Cdc42p required for growth and development of *Saccharomyces cerevisiae*. *Mol Cell Biol* 21, 235–248.
- Mostowy S, Cossart P (2012). Septins: the fourth component of the cytoskeleton. *Nat Rev Mol Cell Biol* 13, 183–194.
- Neufeld TP, Rubin GM (1994). The *Drosophila* peanut gene is required for cytokinesis and encodes a protein similar to yeast putative bud neck filament proteins. *Cell* 77, 371–379.
- Nguyen TQ, Sawa H, Okano H, White JG (2000). The *C. elegans* septin genes, *unc-59* and *unc-61*, are required for normal postembryonic cytokinesis and morphogenesis but have no essential function in embryogenesis. *J Cell Sci* 113, 3825–3837.
- Nonaka H, Tanaka K, Hirano H, Fujiwara T, Kohno H, Umikawa M, Mino A, Takai Y (1995). A downstream target of RHO1 small GTP-binding protein is PKC1, a homolog of protein kinase C, which leads to activation of the MAP kinase cascade in *Saccharomyces cerevisiae*. *EMBO J* 14, 5931–5938.
- Oh Y, Bi E (2010). Septin structure and function in yeast and beyond. *Trends Cell Biol* 21, 141–148.
- Okada H, Abe M, Asakawa-Minemura M, Hirata A, Qadota H, Morishita K, Ohnuki S, Nogami S, Ohya Y (2010). Multiple functional domains of the yeast 1,3-beta-glucan synthase subunit Fks1p revealed by quantitative phenotypic analysis of temperature-sensitive mutants. *Genetics* 184, 1013–1024.
- Okada S, Leda M, Hanna J, Savage NS, Bi E, Goryachev AB (2013). Daughter cell identity emerges from the interplay of *cdc42*, septins, and exocytosis. *Dev Cell* 26, 148–161.
- Ozaki-Kuroda K, Yamamoto Y, Nohara H, Kinoshita M, Fujiwara T, Irie K, Takai Y (2001). Dynamic localization and function of Bni1p at the sites of directed growth in *Saccharomyces cerevisiae*. *Mol Cell Biol* 21, 827–839.
- Peterson EA, Petty EM (2010). Conquering the complex world of human septins: implications for health and disease. *Clin Genet* 77, 511–524.
- Piekny A, Werner M, Glotzer M (2005). Cytokinesis: welcome to the Rho zone. *Trends Cell Biol* 15, 651–658.
- Plomann M, Lange R, Vopper G, Cremer H, Heinlein UA, Scheff S, Baldwin SA, Leitges M, Cramer M, Paulsson M, et al. (1998). PACSIN, a brain protein that is upregulated upon differentiation into neuronal cells. *Eur J Biochem* 256, 201–211.
- Pollard TD, Wu JQ (2010). Understanding cytokinesis: lessons from fission yeast. *Nat Rev Mol Cell Biol* 11, 149–155.
- Prosser DC, Drivas TG, Maldonado-Baez L, Wendland B (2011). Existence of a novel clathrin-independent endocytic pathway in yeast that depends on Rho1 and formin. *J Cell Biol* 195, 657–671.
- Pruliere G, Cosson J, Chevalier S, Sardet C, Chenevert J (2011). Atypical protein kinase C controls sea urchin ciliogenesis. *Mol Biol Cell* 22, 2042–2053.
- Qadota H, Anraku Y, Botstein D, Ohya Y (1994). Conditional lethality of a yeast strain expressing human RHOA in place of RHO1. *Proc Natl Acad Sci USA* 91, 9317–9321.
- Qadota H, Python CP, Inoue SB, Arisawa M, Anraku Y, Zheng Y, Watanabe T, Levin DE, Ohya Y (1996). Identification of yeast Rho1p GTPase as a regulatory subunit of 1,3-beta-glucan synthase. *Science* 272, 279–281.
- Qiu W, Neo SP, Yu X, Cai M (2008). A novel septin-associated protein, Syp1p, is required for normal cell cycle-dependent septin cytoskeleton dynamics in yeast. *Genetics* 180, 1445–1457.
- Rancati G, Crispo V, Lucchini G, Piatti S (2005). Mad3/BubR1 phosphorylation during spindle checkpoint activation depends on both Polo and Aurora kinases in budding yeast. *Cell Cycle* 4, 972–980.
- Reider A, Barker SL, Mishra SK, Im YJ, Maldonado-Baez L, Hurley JH, Traub LM, Wendland B (2009). Syp1 is a conserved endocytic adaptor that contains domains involved in cargo selection and membrane tubulation. *EMBO J* 28, 3103–3116.
- Saarikangas J, Zhao H, Pykalainen A, Laurinmaki P, Mattila PK, Kinnunen PK, Butcher SJ, Lappalainen P (2009). Molecular mechanisms of membrane deformation by I-BAR domain proteins. *Curr Biol* 19, 95–107.
- Schmidt K, Nichols BJ (2004). Functional interdependence between septin and actin cytoskeleton. *BMC Cell Biol* 5, 43.
- Sheff MA, Thorn KS (2004). Optimized cassettes for fluorescent protein tagging in *Saccharomyces cerevisiae*. *Yeast* 21, 661–670.
- Sherman F (1991). Getting started with yeast. *Methods Enzymol* 194, 3–21.
- Shevchenko A, Wilm M, Vorm O, Mann M (1996). Mass spectrometric sequencing of proteins silver-stained polyacrylamide gels. *Anal Chem* 68, 850–858.
- Soufi B, Kelstrup CD, Stoehr G, Frohlich F, Walther TC, Olsen JV (2009). Global analysis of the yeast osmotic stress response by quantitative proteomics. *Mol Biosyst* 5, 1337–1346.
- Srivastava V, Robinson DN (2015). Mechanical stress and network structure drive protein dynamics during cytokinesis. *Curr Biol* 25, 663–670.

- Steels JD, Estey MP, Froese CD, Reynaud D, Pace-Asciak C, Trimble WS (2007). Septin is a component of the mammalian sperm tail annulus. *Cell Motil Cytoskeleton* 64, 794–807.
- Stimpson HE, Toret CP, Cheng AT, Pauly BS, Drubin DG (2009). Early-arriving Syp1p and Ede1p function in endocytic site placement and formation in budding yeast. *Mol Biol Cell* 20, 4640–4651.
- Suetsugu S, Toyooka K, Senju Y (2010). Subcellular membrane curvature mediated by the BAR domain superfamily proteins. *Semin Cell Dev Biol* 21, 340–349.
- Tada T, Simonetta A, Batterton M, Kinoshita M, Edbauer D, Sheng M (2007). Role of septin cytoskeleton in spine morphogenesis and dendrite development in neurons. *Curr Biol* 17, 1752–1758.
- Takeda T, Robinson IM, Savoian MM, Griffiths JR, Whetton AD, McMahon HT, Glover DM (2013). Drosophila F-BAR protein Syndapin contributes to coupling the plasma membrane and contractile ring in cytokinesis. *Open Biol* 3, 130081.
- Tarassov K, Messier V, Landry CR, Radinovic S, Serna Molina MM, Shames I, Malitskaya Y, Vogel J, Bussey H, Michnick SW (2008). An in vivo map of the yeast protein interactome. *Science* 320, 1465–1470.
- Tasto JJ, Morrell JL, Gould KL (2003). An anillin homologue, Mid2p, acts during fission yeast cytokinesis to organize the septin ring and promote cell separation. *J Cell Biol* 160, 1093–1103.
- Taus T, Kocher T, Pichler P, Paschke C, Schmidt A, Henrich C, Mechtler K (2011). Universal and confident phosphorylation site localization using phosphoRS. *J Proteome Res* 10, 5354–5362.
- TerBush DR, Maurice T, Roth D, Novick P (1996). The Exocyst is a multi-protein complex required for exocytosis in *Saccharomyces cerevisiae*. *EMBO J* 15, 6483–6494.
- Tooley AJ, Gilden J, Jacobelli J, Beemiller P, Trimble WS, Kinoshita M, Krummel MF (2009). Amoeboid T lymphocytes require the septin cytoskeleton for cortical integrity and persistent motility. *Nat Cell Biol* 11, 17–26.
- Vetter IR, Wittinghofer A (2001). The guanine nucleotide-binding switch in three dimensions. *Science* 294, 1299–1304.
- Voth WP, Olsen AE, Sbia M, Freedman KH, Stillman DJ (2005). ACE2, CBK1, and BUD4 in budding and cell separation. *Eukaryot Cell* 4, 1018–1028.
- Wach A, Brachat A, Pohlmann R, Philippsen P (1994). New heterologous modules for classical or PCR-based gene disruptions in *Saccharomyces cerevisiae*. *Yeast* 10, 1793–1808.
- Watanabe M, Chen CY, Levin DE (1994). *Saccharomyces cerevisiae* PKC1 encodes a protein kinase C (PKC) homolog with a substrate specificity similar to that of mammalian PKC. *J Biol Chem* 269, 16829–16836.
- Weirich CS, Erzberger JP, Barral Y (2008). The septin family of GTPases: architecture and dynamics. *Nat Rev Mol Cell Biol* 9, 478–489.
- Westfall PJ, Momany M (2002). *Aspergillus nidulans* septin AspB plays pre- and postmitotic roles in septum, branch, and conidiophore development. *Mol Biol Cell* 13, 110–118.
- Wloka C, Nishihama R, Onishi M, Oh Y, Hanna J, Pringle JR, Krauss M, Bi E (2011). Evidence that a septin diffusion barrier is dispensable for cytokinesis in budding yeast. *Biol Chem* 392, 813–829.
- Xie Y, Vessey JP, Konecna A, Dahm R, Macchi P, Kiebler MA (2007). The GTP-binding protein Septin 7 is critical for dendrite branching and dendritic-spine morphology. *Curr Biol* 17, 1746–1751.
- Xue J, Wang X, Malladi CS, Kinoshita M, Milburn PJ, Lengyel I, Rostas JA, Robinson PJ (2000). Phosphorylation of a new brain-specific septin, G-septin, by cGMP-dependent protein kinase. *J Biol Chem* 275, 10047–10056.
- Yamochi W, Tanaka K, Nonaka H, Maeda A, Musha T, Takai Y (1994). Growth site localization of Rho1 small GTP-binding protein and its involvement in bud formation in *Saccharomyces cerevisiae*. *J Cell Biol* 125, 1077–1093.
- Yoshida S, Bartolini S, Pellman D (2009). Mechanisms for concentrating Rho1 during cytokinesis. *Genes Dev* 23, 810–823.
- Yoshida S, Kono K, Lowery DM, Bartolini S, Yaffe MB, Ohya Y, Pellman D (2006). Polo-like kinase Cdc5 controls the local activation of Rho1 to promote cytokinesis. *Science* 313, 108–111.
- Zarrov P, Mazzone C, Mann C (1996). The SLT2(MPK1) MAP kinase is activated during periods of polarized cell growth in yeast. *EMBO J* 15, 83–91.
- Zhang J, Kong C, Xie H, McPherson PS, Grinstein S, Trimble WS (1999). Phosphatidylinositol polyphosphate binding to the mammalian septin H5 is modulated by GTP. *Curr Biol* 9, 1458–1467.
- Zhang H, Macara IG (2008). The PAR-6 polarity protein regulates dendritic spine morphogenesis through p190 RhoGAP and the Rho GTPase. *Dev Cell* 14, 216–226.
- Zhao H, Michelot A, Koskela EV, Tkach V, Stamou D, Drubin DG, Lappalainen P (2013). Membrane-sculpting BAR domains generate stable lipid microdomains. *Cell Rep* 4, 1213–1223.